

## CHAPTER III

### RESULTS AND DISCUSSION

#### 3.1 Extraction of anthocyanins from bran of Thai black rices

Bran of the black rice cultivar Khumdoisakhet, was used to optimize the condition of solvent extraction of anthocyanins. Results of solvent effects on extraction efficiency of anthocyanins from the Thai black rice bran are shown by the corresponding to UV-Vis absorbance of the extracts.

The selection of solvent system for extraction of anthocyanins from the Thai black rice bran was performed by using four different solvents; dichloromethane:methanol (1:4), methanol, methanol containing 0.5% formic acid and, isopropanol, as described in **experimental 2.3.1**. Color of the rice bran extracts obtained by using these four solvents are shown in **Figure 3.1**

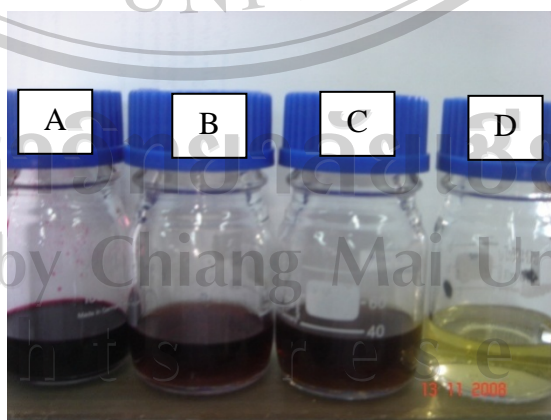


**Figure 3.1** Four extracts of Khumdoisakhet rice bran using; (A) methanol containing 0.5% formic acid, (B) methanol, (C) dichloromethane: methanol (1:4), and (D) isopropanol.

The black rice bran extracts using different solvents showed variations in color due to different content of the extracted anthocyanins. The dark red color has high amount of anthocyanins which was extracted by methanol containing 0.5% formic acid whereas the extract obtained by isopropanol yielded yellow solution indicating a very low amount of anthocyanins. Contents of anthocyanins in these extracts measured by UV-Vis spectrophotometer at 520 nm are shown in **Figure 3.2**. It can be seen that the extract obtained by methanol containing 0.5% formic acid yield the highest amount of anthocyanin components followed by methanol, dichloromethane: methanol (1:4), and isopropanol.

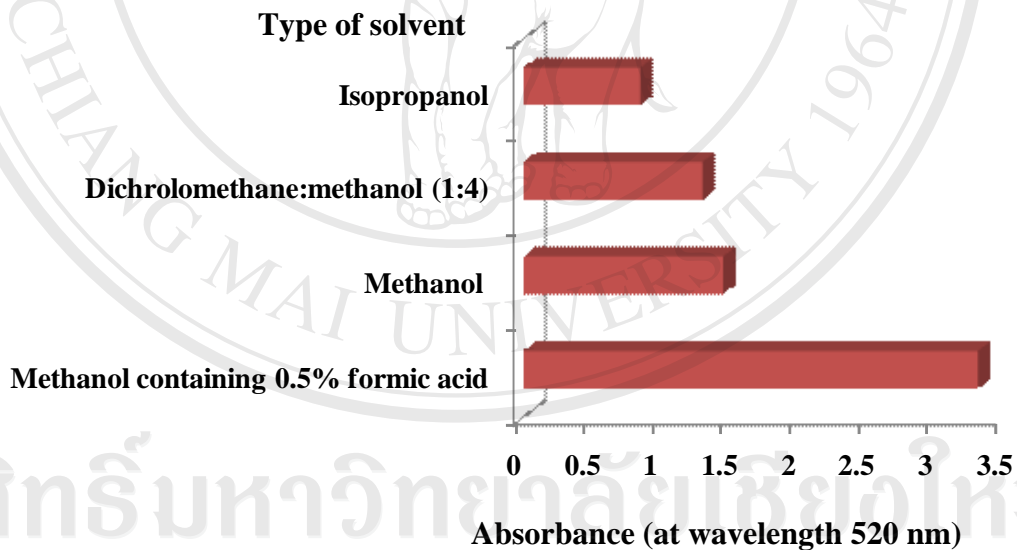


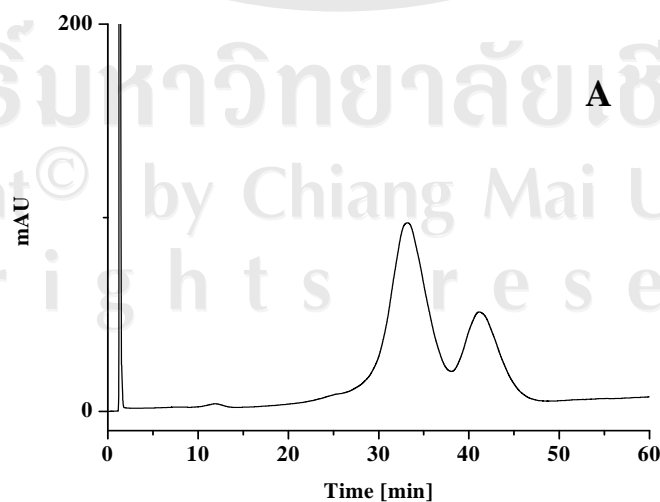
**Figure 3.2** Contents of anthocyanins in the black rice bran extracts expressed by UV-Vis absorbance at wavelength 520 nm.

### 3.2 Separation of anthocyanin components in the black rice bran extract by LC-DAD and LC-ESI-MS

The bran extract of black rice cultivar Khumdoisakheth was used for optimization of the LC-DAD and LC-ESI-MS parameters for the separation of components. Results on the effects of type, composition and flow rate of mobile phase, and column dimension are described below.

#### 3.2.1 Effect of mobile phase composition on component separation

Methanol (MeOH), acetonitrile (MeCN), and water, which are the ordinary solvents used as mobile phase in HPLC system, were used. Previous studies had revealed that the addition of a low amount of acid, for example, acetic acid to the mobile phase could reduce the retention time.<sup>68</sup> Chromatograms obtained from the analysis by LC-DAD of anthocyanin components in the black rice bran extract using different types of mobile phase are shown in **Figure 3.3**.



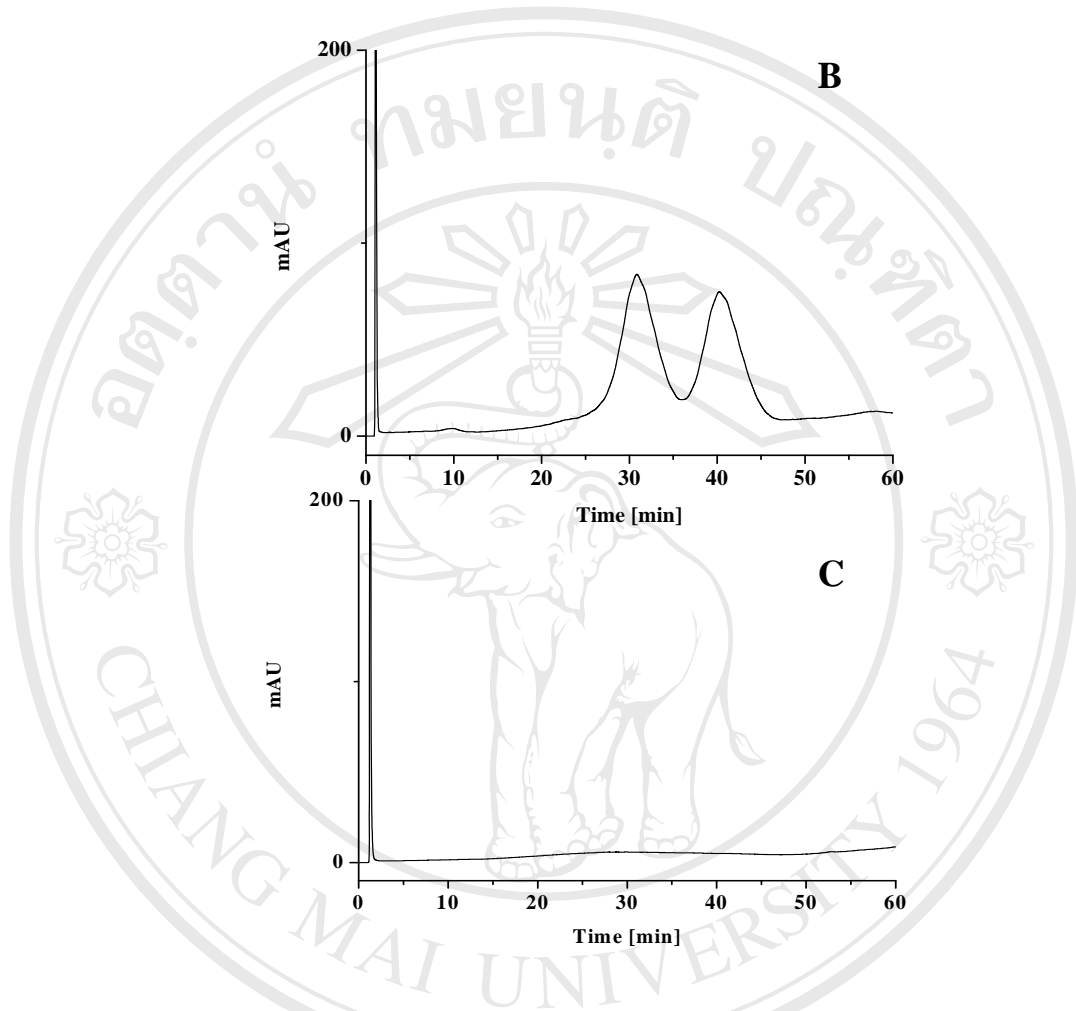


**Figure 3.3** LC-DAD chromatograms (at wavelength 520 nm) of the extract from bran

of Khumdoisakhet rice using (A) methanol: water (90:10), (B) methanol: 0.5 % acetic acid in water (90:10), and (C) acetonitrile : water (90:10) as mobile phase.

Considering the chromatograms of the black rice bran extract using different solvent composition of methanol: 0.5% acetic acid (10:90) and methanol: water (10:90) shown in **Figure 3.3 A and B**, respectively, a similar pattern of component separation was found. However, the better resolution, shorter analysis time and higher

sensitivity of components were observed by the use of methanol: 0.5% acetic acid as mobile phase, whereas the system of acetonitrile: water (10:90) could not elute the components in this condition (see **Figure 3.3 C**).

### 3.2.2 Effect of mobile phase flow rate on component separation

LC-DAD chromatograms (at wavelength 520 nm) of the extract from Khumdoisakheth rice bran using flow rates of mobile phase 0.3 and 0.4 ml/min were shown in **Figure 3.4**. It can be concluded that two different flow rates of mobile phase at 0.3, and 0.4 ml/min yielded similar resolution for separation of components in the rice bran extract, only different in the analysis time. Thus, the flow rate of mobile phase at 0.4 ml/min was selected.

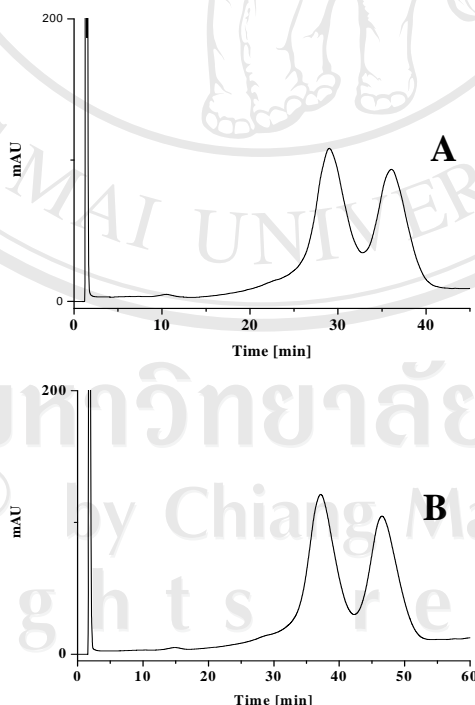


**Figure 3.4** LC-DAD Chromatograms (at wavelength 520 nm) of the extract from bran of Khumdoisakheth rice using (A) 0.3 ml/min and (B) 0.4 ml/min as flow rates of mobile phase.

### 3.2.3 Effect of column dimension on component separation

LC-DAD chromatograms obtained from the separation by Zorbax eclipse plus C<sub>18</sub> (4×100 mm, 3 μm) and Hypersil BDS C<sub>18</sub> (4×100 mm, 3.5 μm) as chromatographic column in HPLC system are shown in **Figure 3.5**.

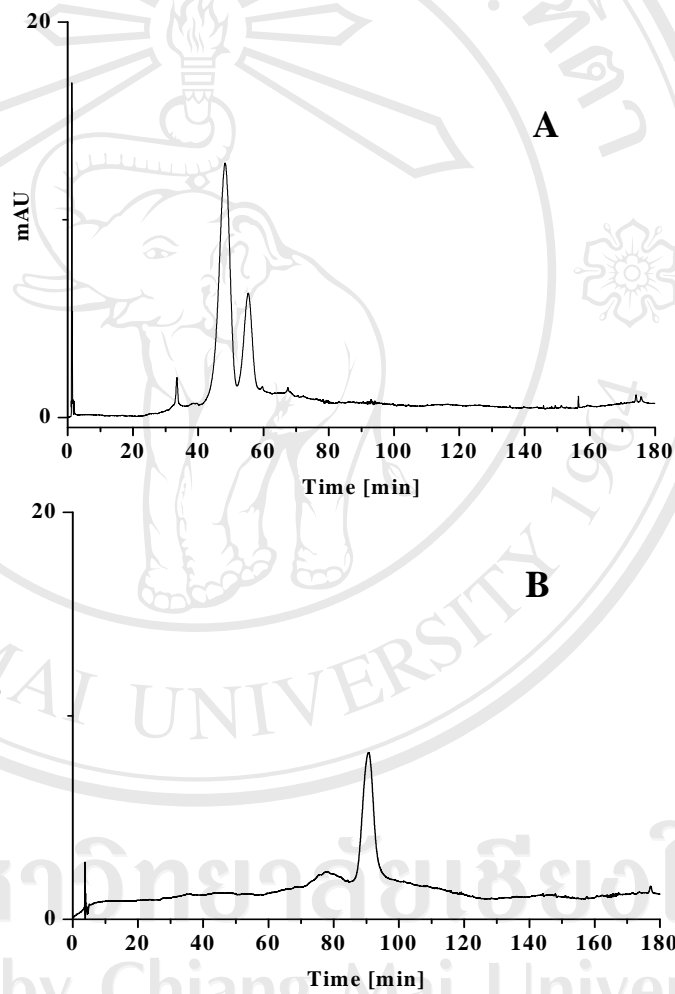
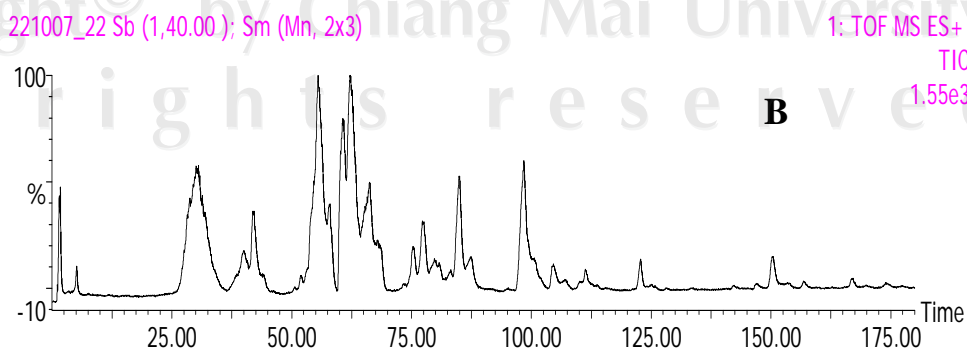
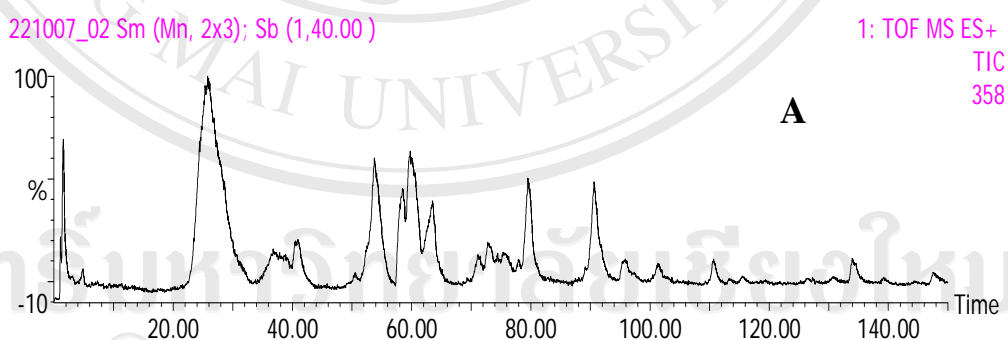


**Figure 3.5** LC-DAD Chromatograms (at wavelength 520 nm) of the extract from bran of Khumdoasakhet rice using (A) Zorbax eclipse plus C<sub>18</sub> (B) Hypersil BDS C<sub>18</sub> as column of the LC system.

LC-DAD chromatograms at wavelength 520 nm of the extract from the bran of Khumdoisakhet rice using Zorbax eclipse plus and Hypersil BDS column showed two peaks of anthocyanin components. The component separation of anthocyanins using small column diameter as shown by the chromatogram in **Figure 3.5 A** is better than that obtained when bigger column diameter was used (**Figure 3.5 B**). A Zorbax eclipse plus C<sub>18</sub> column was then chosen for further analysis of anthocyanin components in the black rice bran extracts. Additionally, this column gave shorter analysis time and higher sensitivity for analysis of anthocyanins.

### 3.2.4 Effect of mobile phase composition on component separation

Chromatograms obtained by LC-ESI-MS of the Khumdoisakhet rice leaf extract at different compositions of mobile phase are shown in **Figure 3.6 A-C**.



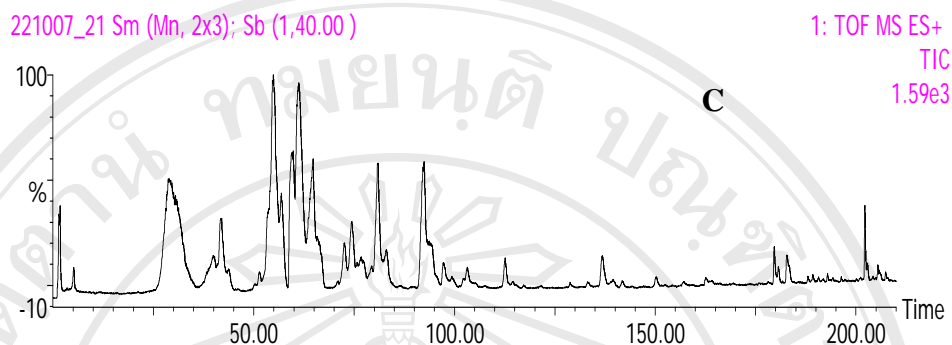


**Figure 3.6** LC-ESI-MS Chromatograms of the extract from the black rice leaves, Khumdoisakhet, using (A) 90% - 50% of 0.5 % acetic acid in water, (B) 90% - 55% of 0.5 % acetic acid in water and (C) 90% - 0% of 0.5 % acetic acid in water mixed with methanol as composition of mobile phase.

It was found that the three chromatograms yielded similar patterns of component separation. The mobile phase composition of 90% - 55% of 0.5 % acetic acid in water mixed with methanol was chosen for further LC-ESI-MS and MS/MS analysis because it yielded the most appropriate resolution and analysis time for the black rice leaf extracts.

#### **Summary of the optimum LC-DAD and LC-ESI-MS conditions**

The optimum LC-DAD and LC-ESI-MS conditions obtained including type of mobile phase, mobile phase composition and flow rate, and column dimension are listed in **Table 3.1**. These optimum conditions were used in further experiments.

**Table 3.1** The optimum LC-DAD and LC-ESI-MS conditions.

Operation	Optimal conditions
Column	Zorbax eclipse plus C <sub>18</sub> (4×100 mm, 3 μm)
Mobile phase	A; methanol B; 0.5 % acetic acid in water
Compositions mobile phase gradient system	90% - 55% of 0.5 % acetic acid in water : methanol
Flow rate of mobile phase	0.4 ml/min
Wavelength of DAD	520 nm

### 3.3 Identification of anthocyanins in the black rice extracts by LC-DAD, LC-ESI-MS and LC-ESI-MS/MS

#### 3.3.1 Optimization of electrospray ionization mass spectrometry (ESI-MS) parameters for analysis of the anthocyanin standards

Parameters of the ESI-MS ionization technique have great effects on the component separation and the ESI-MS performance in term of fragmentation and sensitivity for analysis of the compounds of interest. These parameters are fragmentor voltage, capillary voltage, drying gas temperature, drying gas flow rate, and nebulizer pressure.

##### 3.3.1.1 Fragmentor voltage in positive ionization mode

By varying fragmentor voltage at 110, 120, 130, 140, and 150 V, the most appropriate peak area and ion count useful for detection of cyanidin-3-*O*-glucoside as well as other anthocyanins was obtained. Total ion chromatograms (TICs) of cyanidin-3-*O*-glucoside obtained by varying fragmentor voltage at every 2-minute step are shown in **Figure 3.7**.

At each fragmentor voltage, peak area and ion count of cyanidin-3-*O*-glucoside were calculated from its corresponding TICs and mass spectra, respectively, and are listed in **Table 3.2**.

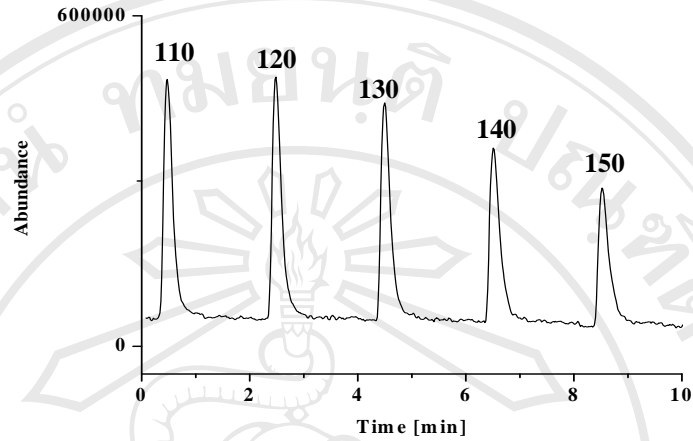


**Figure 3.7** TICs of cyanidin-3-*O*-glucoside at fragmentor voltage 110, 120, 130, 140, and 150 V in positive ionization mode.

**Table 3.2** Peak areas and ion counts of cyanidin-3-*O*-glucoside at varied fragmentor voltages in positive ionization mode

Fragmentor voltage [V]	Peak area*	Ion count
110	5444320	233976
120	5246360	122384
130	480680	63534
140	407749	65062
150	345535	40862

\* obtained by integrator

Fragmentor voltage is an important parameter. It is the first parameter that should be optimized for good sensitivity of detection and appropriate fragmentation pattern. Fragmentor voltage also affected the fragmentation of sample ions. High fragmentor voltage can cause fragmentation to occur which provides structural information of the ion. In general, high fragmentor voltage helps the capillary and the entrance of the skimmer. For compounds that do not fragment easily, higher fragmentor voltage often results in better ion transmission. Data of peak areas and ion counts of cyanidin-3-*O*-glucoside at different fragmentor voltages shown in **Table 3.2** reveal that at fragmentor voltage 110 V, a useful pattern of mass spectrum was obtained. Thus fragmentor voltage at 110 was used for further optimization of other parameter for sensitivity of detection.

### 3.3.1.2 Capillary voltage in positive ionization mode

By varying capillary voltage at 3000, 3500, 4000, 4500 and 5000 V, the most appropriate peak areas and ion count useful for identification of cyanidin-3-*O*-glucoside as well as other anthocyanins was obtained. The TICs of cyanidin-3-*O*-glucoside obtained by varying capillary voltage at every 2-minute step are shown in

#### **Figure 3.8.**

At each capillary voltage, peak areas and ion counts of cyanidin-3-*O*-glucoside were calculated from its corresponding TICs and mass spectra, respectively, and are as listed in **Table 3.3**.

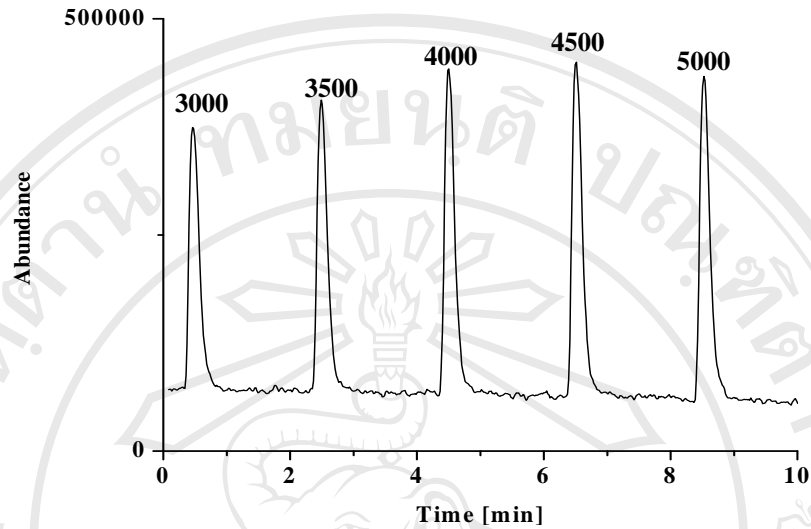


**Figure 3.8** TICs of cyanidin-3-*O*-glucoside at capillary voltage 3000, 3500, 4000, 4500, and 5000 V in positive ionization mode.

**Table 3.3** Peak areas and ion counts of cyanidin-3-*O*-glucoside at varied capillary voltages in positive ionization mode

Capillary voltage [V]	Peak area*	Ion count
3000	3415390	217008
3500	3688830	68264
4000	4219130	188720
4500	4371060	252208
5000	4201470	218348

\*obtained by integrator

The capillary voltage is applied to the inlet of the capillary and influences the transmission of the ion through the capillary sampling orifice. To establish the optimal capillary voltage, in this study the parameter was varied at 3000, 3500, 4000, 4500 and 5000 V. The most appropriate of mass spectrum pattern appeared at capillary voltage 3500 V. Although, the capillary voltage at 4500 V gave the highest sensitivity (peak area), an increased cost of operation was anticipated. Thus capillary voltage at 3500 V was chosen for detection of anthocyanins.

#### 3.3.1.3 Drying gas temperature in positive ionization mode

By varying drying gas temperature at 300, 310, 320, 330, 340 and 350 °C, the most appropriate peak areas and ion count useful for detection of cyanidin-3-*O*-glucoside as well as other anthocyanins was obtained. The TICs of cyanidin-3-*O*-glucoside obtained by varying drying gas temperature at every 2-minute step are shown in **Figure 3.9**.

At each drying gas temperature, peak area and ion count of cyanidin-3-*O*-glucoside were calculated from its corresponding TICs and mass spectra, respectively, and are listed in **Table 3.4**.

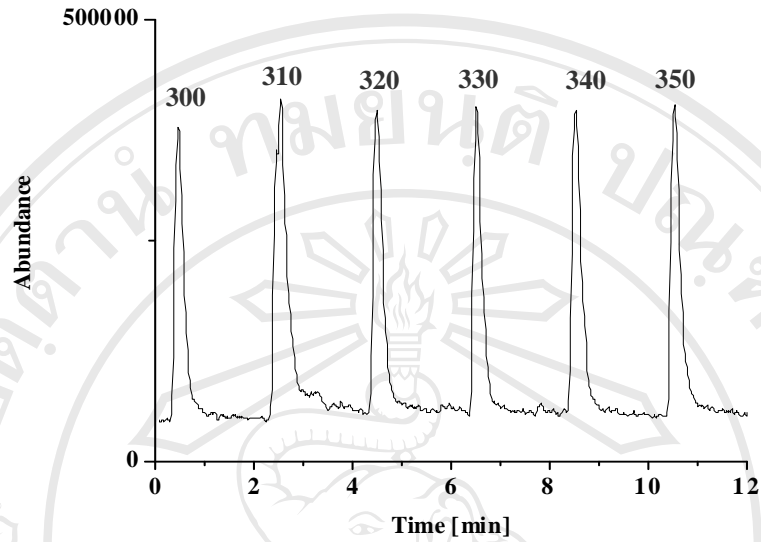


**Figure 3.9** TICs of cyanidin-3-*O*-glucoside at drying gas temperature 300, 310, 320, 330, 340 and 350 °C in positive ionization mode.

**Table 3.4** Peak areas and ion counts of cyanidin-3-*O*-glucoside at varied drying gas temperatures in positive ionization mode

Drying gas temperature [°C]	Peak areas*	Ion count
300	3830000	79182
310	5825830	26984
320	4488230	114406
330	4158950	106422
340	4718140	82574
350	4778000	122014

\*obtained by integrator

The optimum drying gas temperature can be different for each group of compounds. Drying efficiency is generally a function of the organic nature of the spray, the more organic solvent in the spray the faster it will evaporate at a lower drying gas temperature. Generally, use as low a drying temperature as possible in order to avoid thermal degradation of the compounds of interest is preferred. Sometime, for some compounds, higher temperatures will actually increase ionization of more molecules in the gas phase so each compound will need to be evaluated over a range of temperature. Peak areas and ion counts of cyanidin-3-*O*-glucoside at various values of drying gas temperature (300, 310, 320, 330, 340 and 350 °C) are shown in **Table 3.4**. Drying gas temperature at 350 °C gave the highest peak areas and ion counts which indicated that this value of drying gas temperature is the optimum value for sensitivity of detection.

#### **3.3.1.4 Drying gas flow rate in positive ionization mode**

By varying drying gas flow rate at 8, 9, 10, 11 and 12 l/min, the most appropriate peak areas and ion count useful for detection of cyanidin-3-*O*-glucoside as well as other anthocyanins was obtained. The TICs of cyanidin-3-*O*-glucoside obtained by varying drying gas flow rate at every 2-minute step are shown in **Figure 3.10**.

At each drying gas flow rate, peak area and ion count of cyanidin-3-*O*-glucoside were calculated from its corresponding TICs and mass spectra, respectively, and are as listed in **Table 3.5**.

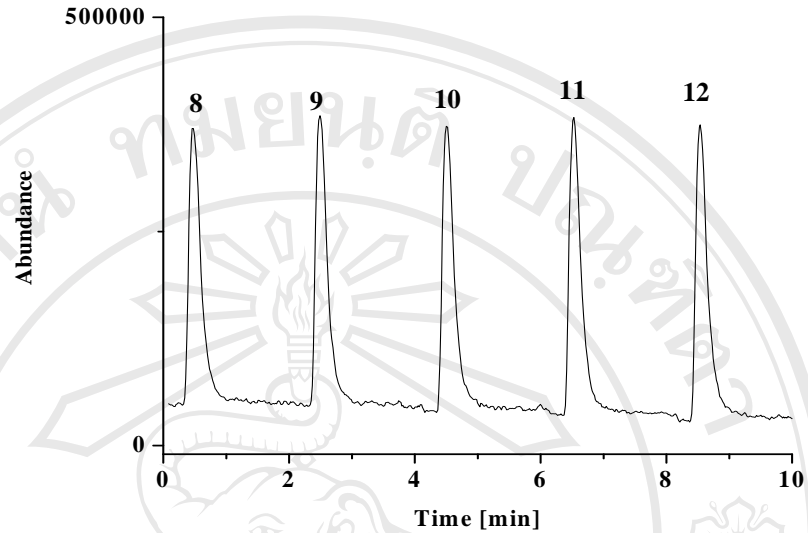


**Figure 3.10** TICs of cyanidin-3-*O*-glucoside at drying gas flow rate 8, 9, 10, 11 and 12 l/min in positive ionization mode.

**Table 3.5** Peak areas and ion counts of cyanidin-3-*O*-glucoside at varied drying gas flow rates in positive ionization mode

Drying gas flow rate [l/min]	Peak areas*	Ion count
8	4341690	60140
9	4408660	67164
10	4564850	101370
11	4604730	102314
12	4607110	102794

\*obtained by integrator

This parameter controls the flow rate of nitrogen drying gas. The flow rate required depends on the parameter of analysis, which are the HPLC flow rate and the drying gas temperature. In general, the higher the HPLC flow rate the higher the drying gas flow rate is needed. Effect of the drying gas flow rate on the signal intensity was evaluated in rang 8-12 l/min at 8, 9, 10, 11 and 12 l/min. It was shown that signal intensity dramatically increased as increasing of drying gas flow rate, and the 12 l/min of drying gas flow rate is the most appropriate for sensitivity of detection of anthocyanin compounds.

#### **3.3.1.5 Nebulizer pressure in positive ionization mode**

By varying nebulizer pressure at 26, 28, 30, 32, and 34 psi, the most appropriate peak areas and ion count useful for detection of cyanidin-3-*O*-glucoside as well as other anthocyanins was obtained. The TICs of cyanidin-3-*O*-glucoside obtained by varying nebulizer pressure at every 2-minute step are shown in **Figure 3.11**.

At each nebulizer pressure, peak area and ion count of cyanidin-3-*O*-glucoside were calculated from its corresponding TICs and mass spectra, respectively, and are as listed in **Table 3.6**.

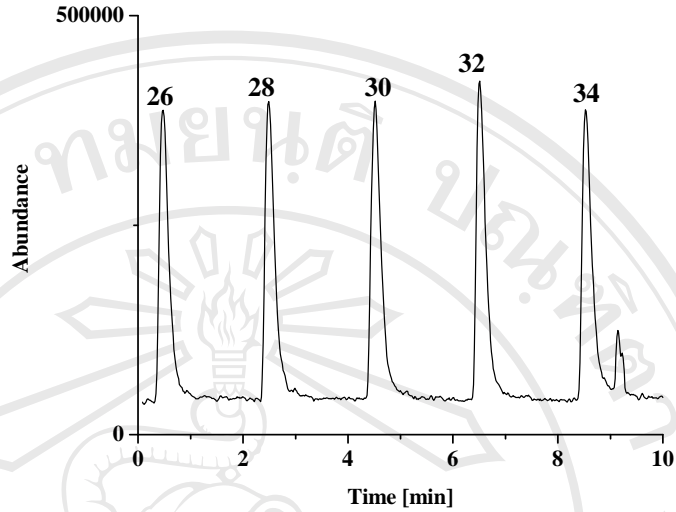


**Figure 3.11** TICs of cyanidin-3-*O*-glucoside at nebulizer pressure 26, 28, 30, 32, and 34 psi in positive ionization mode.

**Table 3.6** Peak areas and ion counts of cyanidin-3-*O*-glucoside at varied nebulizer pressures in positive ionization mode.

Nebulizer pressure [psi]	Peak areas*	Ion count
26	4359980	67962
28	4565190	69339
30	4523910	67283
32	4589350	113203
34	4437700	96339

\* obtained by integrator

This parameter controls the pressure of the nitrogen nebulizing gas. The pressure required is set as a function of the HPLC flow rate, the mobile phase composition, and the ionization mode. A variation of intensity of the analyte was observed when a nebulizer pressure was varied at 26, 28, 30, 32, and 34 psi. The nebulizer pressure at 30 psi yielded the highest appropriate of peak areas and ion counts of cyanidin-3-*O*-glucoside.

#### Summary of the optimum LC-ESI-MS conditions

For LC-ESI-MS analysis of black rice anthocyanins, cyanidin-3-*O*-glucoside was used to optimize the electrospray ionization parameters such as fragmentor voltage, capillary voltage, drying gas flow, drying gas temperature, and nebulizer pressure. The optimum values of these parameters are summarized in **Table 3.7**.

**Table 3.7** The optimum ESI-MS condition for analysis of anthocyanins.

Operation parameter	Optimal condition
Quadrupole temperature	100 °C
Fragmentor voltage	110 V
Capillary voltage	3500 V
Drying gas temperature	350 °C
Drying gas flow rate	12 l/min
Nebulizer pressure	30 psi

### 3.3.2 Optimization of collision energy in CID process for the identification of anthocyanin components

#### 3.3.2.1 Optimization of collision energy for the identification of anthocyanin-3-*O*-monoglucoside

As pattern of fragmentation of the parent ion of interest in MS/MS operation is mainly due to the energy of collision gas (collision energy) used in the CID process. Varying collision energy at 15, 17, 20, and 22 was performed to obtain the most appropriate pattern of product ion mass spectra useful for component identification. The product ion mass spectra of malvidin-3-*O*-glucoside used as standard compound having parent ion at  $m/z$  493 in positive ionization mode were obtained as shown in

**Figure 3.12.**

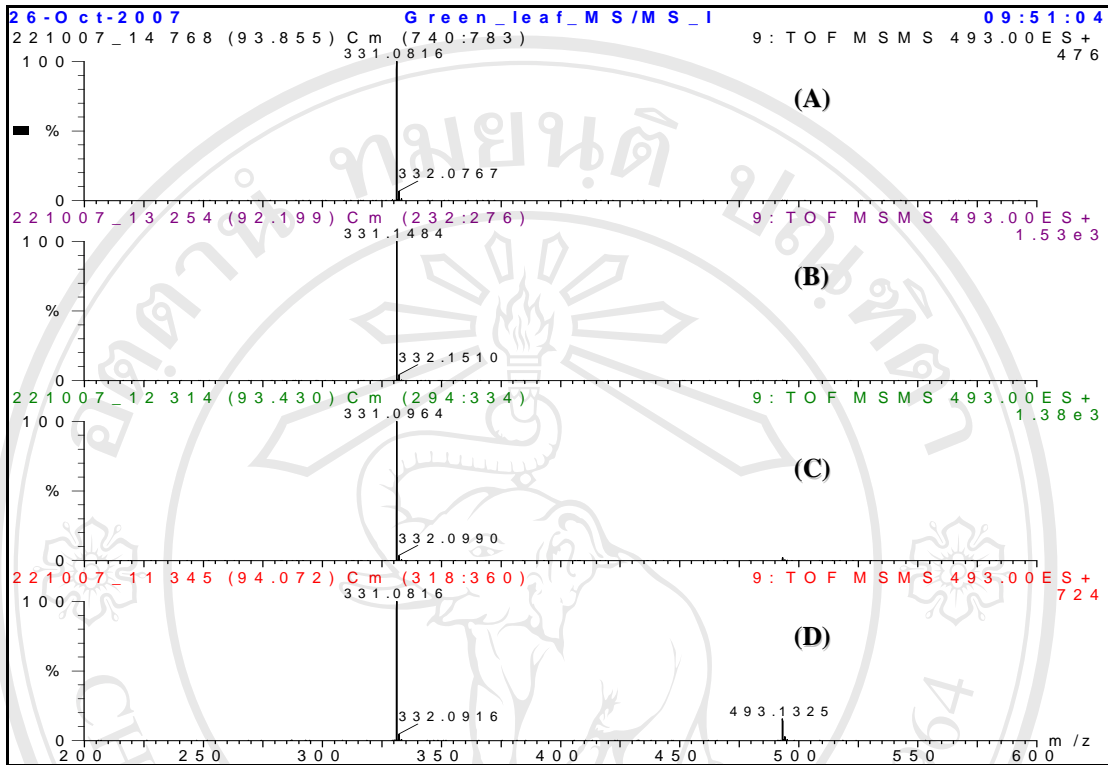


**Figure 3.12** Product ion mass spectra of malvidin-3-*O*-glucoside obtained by LC-ESI-MS/MS (Q-TOF) of ion at  $m/z$  493 using collision energy of (A) 22 V, (B) 20 V, (C) 17 V, and (D) 15 V.

The parent and product ion of malvidin-3-*O*-glucoside obtained by varying collision energy at 15, 17, 20 and 22 V consisted of  $m/z$  463 and 331, respectively, which corresponding to the loss of a glucose (162 Da). The collision energy at 15 V yielded both parent and product ions, whereas the collision energy at 17, 20, and 22 V gave only product. Although the maximum value of ion counts of malvidin-3-*O*-glucoside achieved at the collision energy of 20 V, collision energy at 15 V was more appropriate for component identification.

### 3.3.2.2 Optimization of collision energy for the identification of anthocyanin-3-*O*-diglucoside

The anthocyanins-3-*O*-diglucoside studied in this experiment was cyanidin-3-*O*-xyloside glucoside having molecular ion in positive ionization mode at  $m/z$  581. By varying collision energy at 15, 17, 20, 22, and 25 V, the corresponding product ion mass spectra of cyanidin-3-*O*-xyloside glucoside were obtained as shown in **Figure 3.13**.

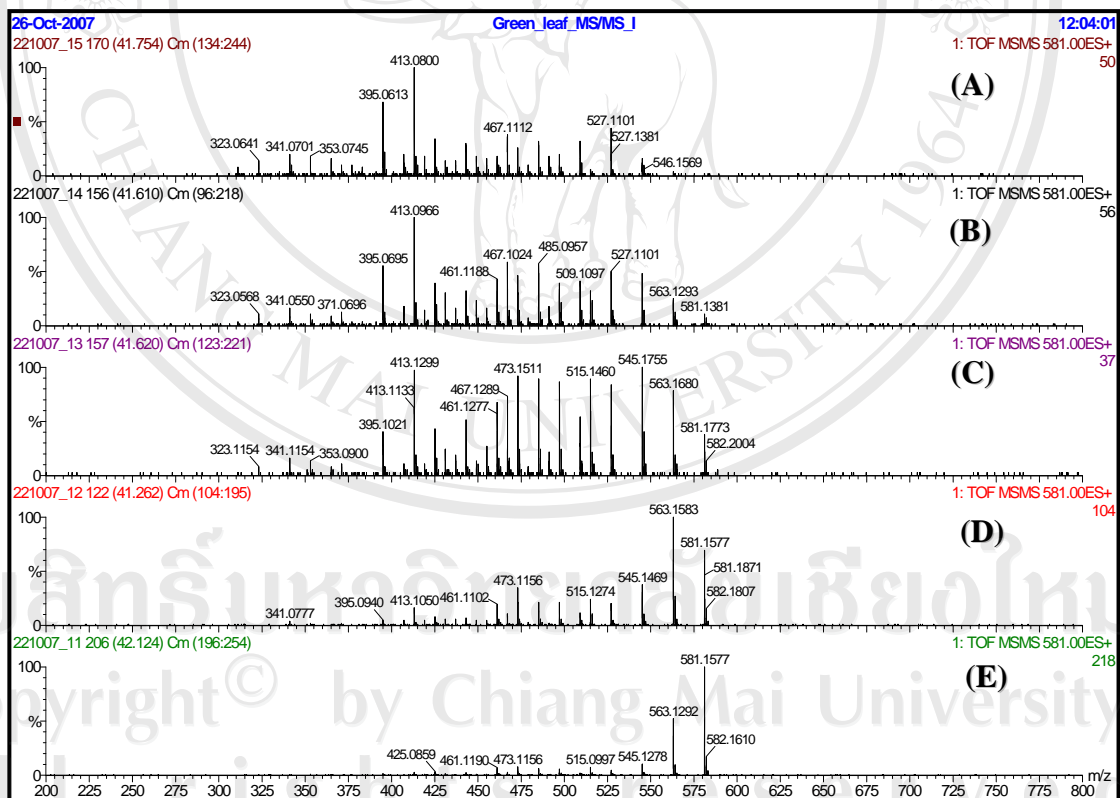


**Figure 3.13** Product ion mass spectra of cyanidin-3-*O*-xyloside glucoside obtained by LC-ESI-MS/MS (Q-TOF) of ion at  $m/z$  581 using collision energy of (A) 25 V, (B) 22 V, (C) 20 V, (D) 17 V and (E) 15 V.

As the results, the ion at  $m/z$  413 was the base peak in the mass spectra obtained by using collision energy of 20, 22 and 25 V. Additionally, the dominant ion at  $m/z$  395, 527, 467, 353, 341 and 323 were also observed in these mass spectra. However, The parent ion at  $m/z$  581 was not present in these spectra which resulted from too high collision energy. At lower collision energy of 15 and 17 V, the base peaks were shifted to ion at  $m/z$  563  $[M-H_2O]^+$  and 581 $[M]^+$ , respectively. A collision energy of 20 V gave the most appropriate mass spectral pattern regardless of the ion count, which indicated that this value was useful for component identification.

### 3.3.2.3 Optimization of collision energy for identification of anthocyanin-3-*O*-diglucoside-5-*O*-glucoside and anthocyanin-3-*O*-acylate-glucoside.

In groups of anthocyanin-3-*O*-diglucoside-5-*O*-glucoside and anthocyanin-3-*O*-acylate-glucoside, the parent ion at  $m/z$  757 of cyanidin-3-*O*-(*p*-coumaroyl)glucoside-5-*O*-glucoside was used for optimization of CID process. By varying collision energy at 15, 17, 20, 22, and 25 V, the product ion mass spectra of cyanidin-3-*O*-(*p*-coumaroyl)glucoside-5-*O*-glucoside were obtained as shown in **Figure 3.14**.

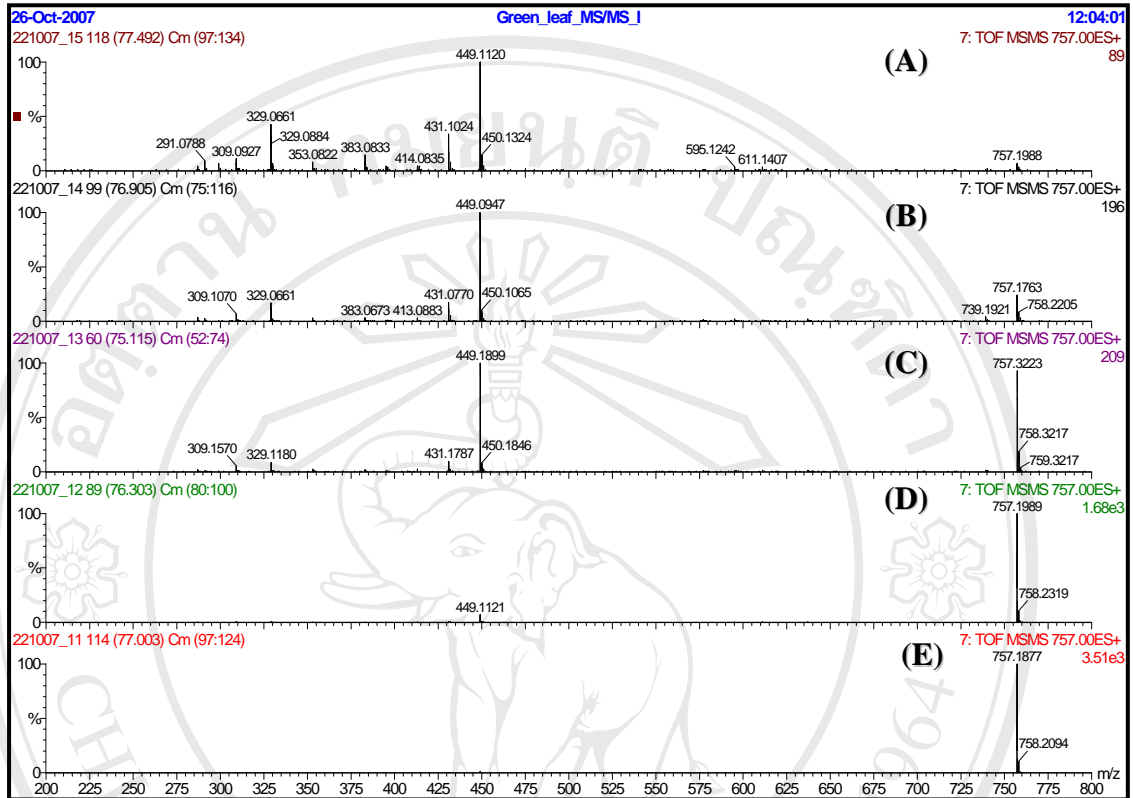


**Figure 3.14** Product ion mass spectra of cyanidin-3-*O*-(*p*-coumaroyl)glucoside-5-*O*-glucoside obtained by LC-ESI-MS/MS (Q-TOF) of ion at  $m/z$  757 using collision energy of (A) 25 V, (B) 22 V, (C) 20 V, (D) 17 V, and (E) 15 V.

A collision energy of 25 V yielded the product ions at  $m/z$  291, 329, 383, 431, 449, 595 and 611. Relatively abundant Y type ion was observed at  $m/z$  449 ( $Y_1^+$ ) corresponding to cyanidin-3-*O*-glucoside, whereas other ions at  $m/z$  431 and 329 formed by common fragmentation routes were also present. An ion at  $m/z$  329 can be considered as a characteristic of the 1-2 interglycosidic linkage in 3-*O*-glycoside adducts. Addition fragment ion at  $m/z$  353 was also observed. While the mass spectra

obtained using collision energy at 15, 17, 20 and 22 V yielded the product ions with higher masses at  $m/z$  309, 329 and 449. Therefore, collision energy at 25 V gave the most appropriate mass spectral pattern of product ions which indicated that this value was the optimum value for obtaining a mass spectrum useful for structural identification of cyanidin-3-*O*-(*p*-coumaroyl)glucoside-5-*O*-glucoside.

**Table 3.8** compiles the optimum collision energies used in CID process of each anthocyanin groups. These collision energies were used in further experiments.

**Table 3.8** The optimum collision energies of each anthocyanin groups.

Group type of anthocyanins	Optimal collision energy (eV)
anthocyanins-3- <i>O</i> -glucoside (monoglucoside)	15
anthocyanins-3- <i>O</i> -diglucoside	20
anthocyanins-3- <i>O</i> -diglucoside-5- <i>O</i> -glucoside and anthocyanins-3- <i>O</i> -acylate-glucoside	25

### 3.3.3 Identification of anthocyanins in the black rice leaf, seed and bran extracts by LC-DAD, LC-ESI-MS and LC-ESI-MS/MS

Identification of anthocyanins in the Thai black rice leaf, seed and bran extracts was performed by using HPLC coupled with diode array detector (DAD), electrospray ionization mass spectrometer (ESI) and hybrid quadrupole time-of-flight mass spectrometer with collision-induced dissociation (CID).

#### 3.3.3.1 Anthocyanins identified by LC-DAD

Reversed-phase LC is the most common method used for the separation of anthocyanins. Detection is usually performed using UV diode-array absorbance detection (DAD). The UV-Vis spectra of anthocyanins can give information on the nature of the aglycone, glycosylation pattern, and possibility of acylation. Single wavelength detectors can selective monitor anthocyanins between 520 and 546 nm, where no other plant phenolics show absorption at these wavelengths.<sup>69</sup> LC-DAD chromatograms at wavelength 520 nm of extract from bran of the black rice cultivar Khumdoisakhet possessed two dominant peaks which indicated the retention time of anthocyanin components (**Figure 3.15**). The UV-Vis spectra of anthocyanins obtained from LC-DAD of an extract from bran of the Khumdoisakhet rice are shown in **Figure 3.16**.

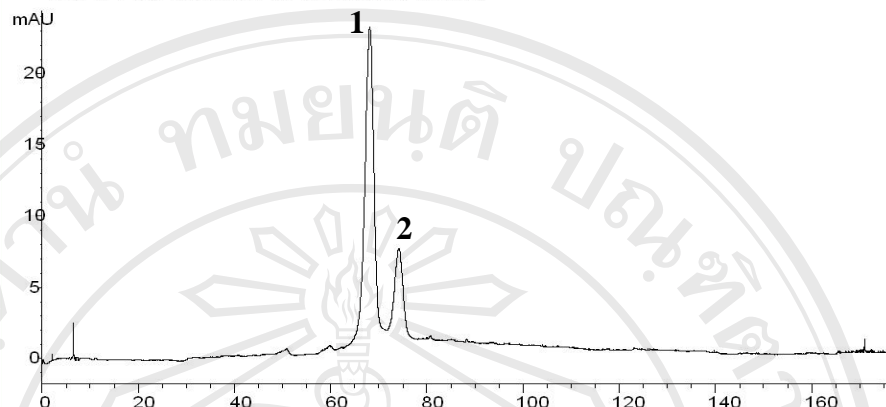


**Figure 3.15** Chromatogram obtained by LC-DAD at wavelength 520 nm of an extract from bran of the Khumdoisakhet rice.

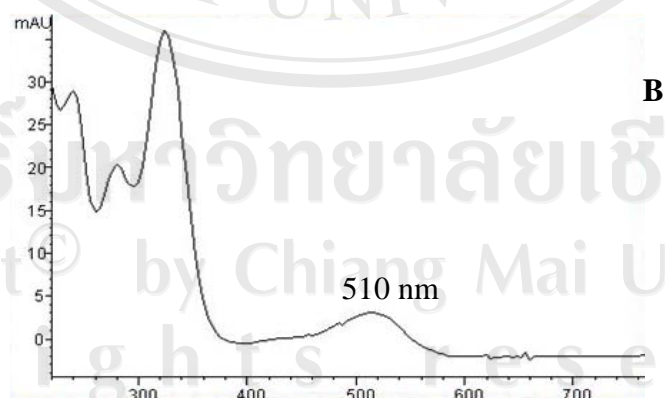
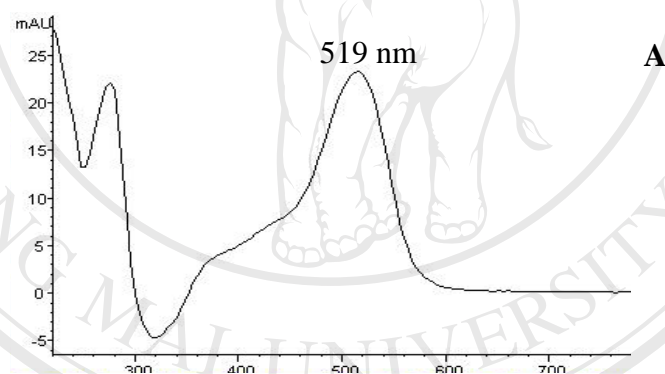


**Figure 3.16** UV-Vis spectra obtained by LC-DAD of an extract from bran of the Khumdoisakhet rice (A) Peak 1 and (B) Peak 2, of which their chromatogram is shown in **Figure 3.15**.

### 3.3.3.2 Anthocyanins identified by LC-ESI-MS

The mass spectrum of anthocyanins obtained from LC-ESI-MS of the Khumdoisakhet rice bran extracts possessed molecular ion  $[M]^+$  at  $m/z$  449 and a fragmented ion at  $m/z$  287 which corresponding to loss of a glucose moiety (162 Da) from the molecular ion (**Figure 3.17**). The fragment ion of  $m/z$  287 was equal the molecular ion of cyanidin aglycone. This anthocyanin was thus identified as cyanidin-3-*O*-glucoside.

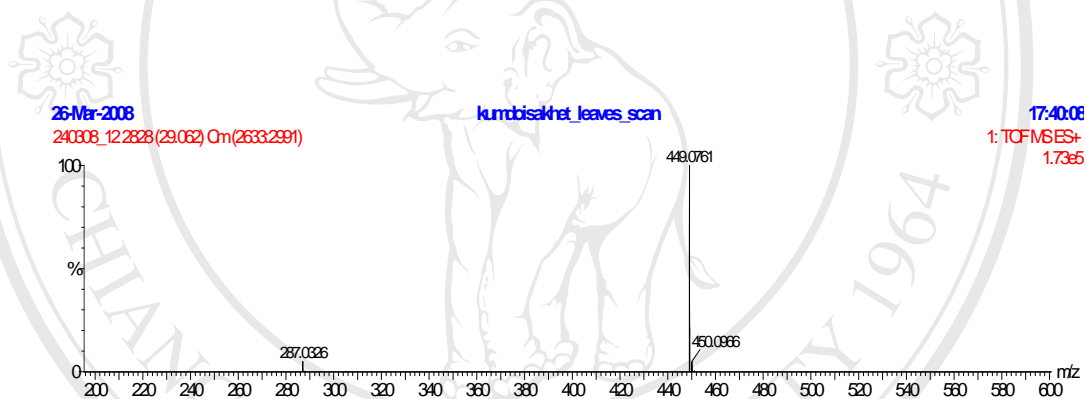


**Figure 3.17** Full scan ESI-MS spectrum of cyanidin-3-*O*-glucoside having molecular ion at  $m/z$  449.

The extracted ion chromatogram (mass chromatogram) at  $m/z$  449 shown in

**Figure 3.18 A** indicated the present of cyanidin-3-*O*-glucoside (MW 449) at retention time 29.02 min, which also appears in the TIC of the rice bran extract (**Figure 3.18 B**).

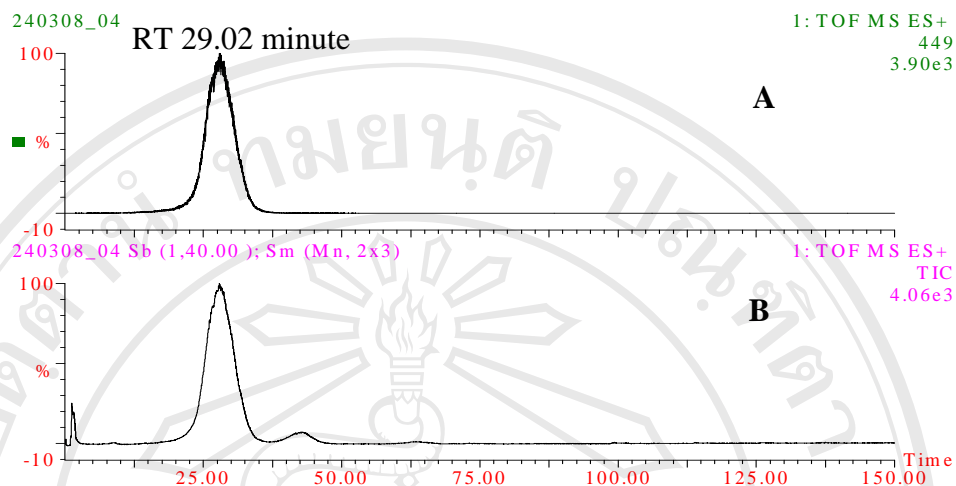


**Figure 3.18** Chromatograms obtained from LC-ESI-MS of bran extract of Khumdoisakhet rice; (A) Mass chromatogram at  $m/z$  449 (B) Total ion chromatogram.

### 3.3.3.3 Anthocyanins identified by LC-ESI-MS/MS

Since there was not much detail of fragmentation obtained from ESI-MS spectrum of single mass spectrometer, the structures of compounds of interest could not be identified. So that product ion scan must be performed from the second mass spectrometer and can be useful due to the variety patterns of mass spectra which depend on the different structures of compounds. Moreover, characteristic ions were also used for structural identification of each group of compounds.

The Thai black rice extracts were introduced into electrospray ionization source of the MS/MS by LC using the optimized LC-ESI-MS condition and the results of their mass spectra were obtained. The TICs chromatograms resulted from LC-ESI-MS analysis of the extracts from leaves, seeds and brans of the black rice cultivars BGMSN11 and Khumdoisakhet are shown in **Figure 3.19-3.21**, respectively. These

anthocyanins were co-eluted with other components in the extracts and could be screened by LC-ESI-MS using the mass chromatogram technique to position the retention time of anthocyanin ions. Then LC-ESI-MS/MS analysis of anthocyanins resulting in dissociation of parent ion to yield informative mass spectra would aid the identification of these compounds in the black rice sample extracts.

An example is shown by the full-scan ESI-MS spectrum of cyanidin-3-*O*-glucoside-5-*O*-rhamnoside in **Figure 3.22 A** compared with at obtained from ESI-MS/MS in **Figure 3.22 B**. Both technique gave a molecular ion of cyanidin-3-*O*-glucoside-5-*O*-rhamnoside at  $m/z$  595, but only MS/MS spectrum possesses the fragment ion at  $m/z$  449  $[M-146]^+$  and 287  $[M-146-162]^+$  which obtained by the loss of rhamnose (146 Da) followed by glucose (162 Da), respectively. The fragment ion at  $m/z$  287 indicated an aglycone of this anthocyanin is cyanidin.

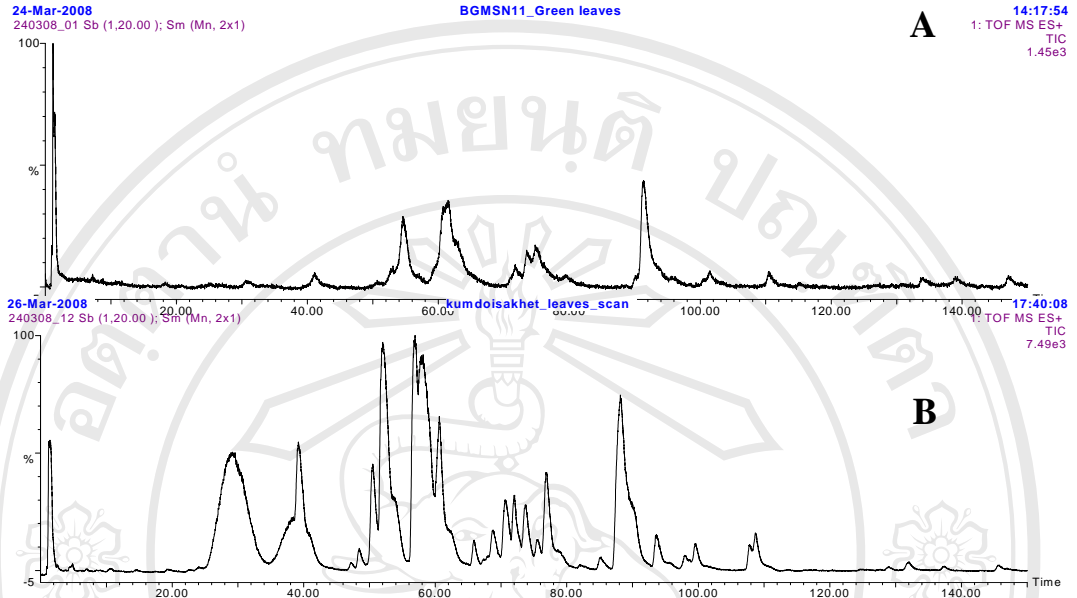


**Figure 3.19** Chromatograms obtained from LC-ESI-MS of extracts from leaves of two black rice cultivars; (A) BGMSN 11 (B) Khumdoisakhet.

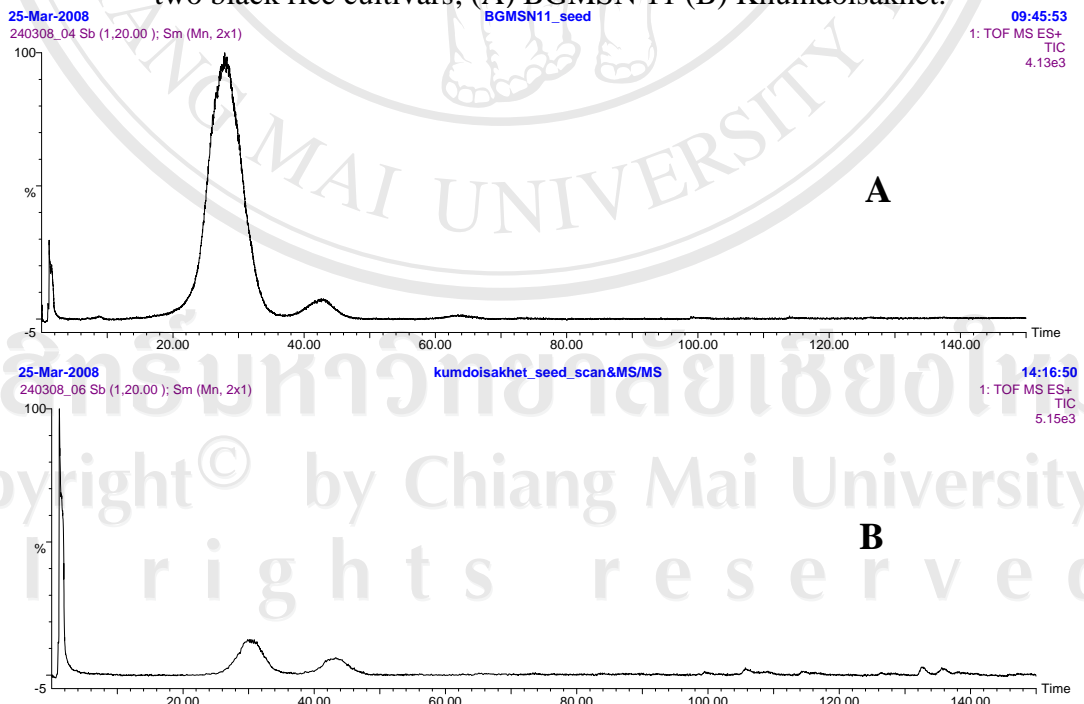


**Figure 3.20** Chromatograms obtained from LC-ESI-MS of extracts from seed of two black rice cultivars; (A) BGMSN 11 (B) Khumdoisakhet.

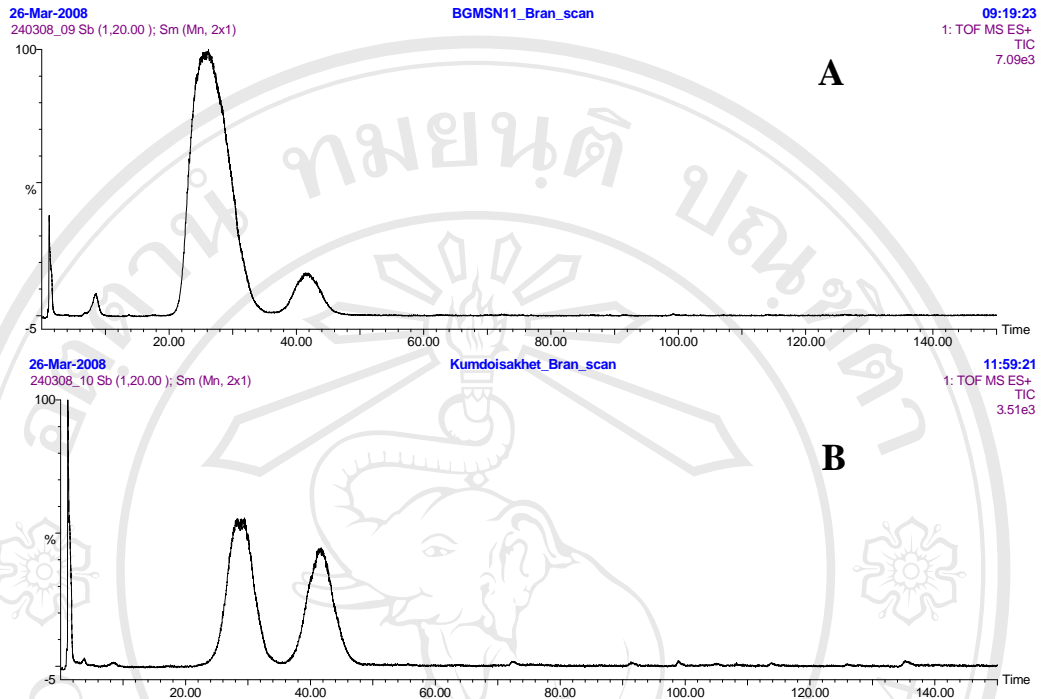


**Figure 3.21** Chromatograms obtained from LC-ESI-MS of extracts from bran of two black rice cultivars; (A) BGMSN 11 (B) Khumdoisakhet.

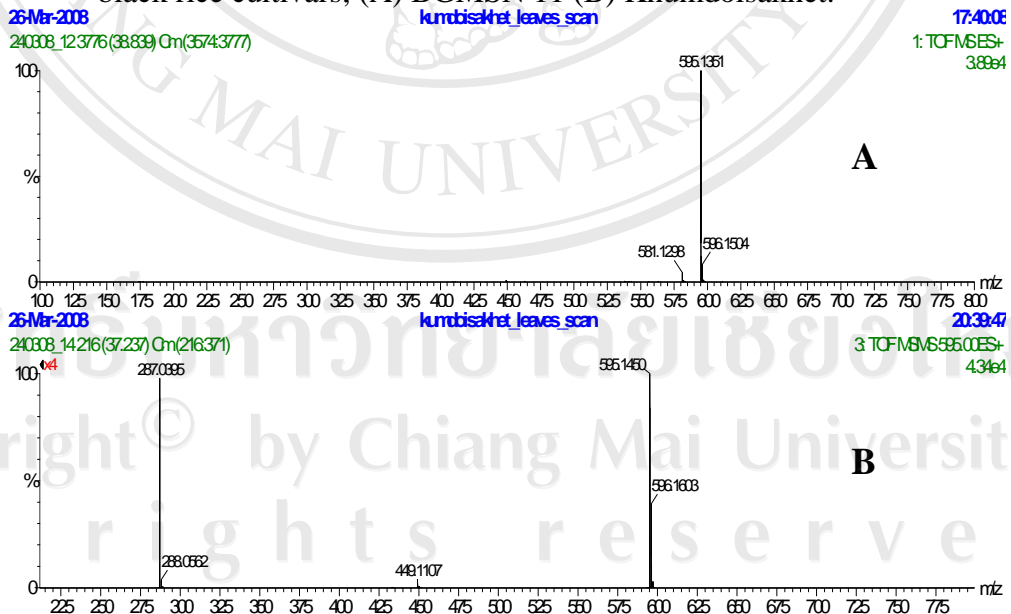


**Figure 3.22** ESI-MS and ESI-MS/MS spectrum of cyanidin-3-*O*-glucoside-5-*O*-rhamnoside having molecular ion at  $m/z$  595 obtained from of the Thai black rice extract; (A) ESI-MS (B) ESI-MS/MS.

#### 3.3.3.4 Anthocyanins in bran of the Thai black rice

The ESI-MS/MS operation was performed by applying an appropriate energy (collision energy) via argon gas for collision-induced dissociation to the selected mass ion. The selected mass ion was dissociated into small mass ions showing a characteristic of dissociation pattern or fingerprint of each anthocyanin on mass spectrum. Results of the UV-Vis band obtained by DAD, the full-scan mass spectra obtained by ESI-MS and the full-scan MS/MS spectra of the selected mass ions of anthocyanin components in the black rice sample extracts were used for structural identification of this group of compounds as follows:

##### **Cyanidin-3-*O*-glucoside**

Total ion chromatogram (TIC) and mass chromatogram at  $m/z$  449 obtained from LC-ESI-MS of extracts from seed and bran of the black rice cultivars Khumdoisakhet are presented in **Figure 3.23**. The molecular ion at  $m/z$  449 was detected at retention time 29.02 min as shown in the mass chromatogram. Full scan ESI-MS spectrum obtained from LC-ESI-MS of the extracts shown in **Figure 3.24 A** indicated the molecular ion of cyanidin glucoside (MW 449). The parent ion at  $m/z$  449 was selected as a precursor ion for CID operation by argon gas in order to achieve the ESI-MS/MS spectrum which gave the dissociation of cyanidin glucoside (**Figure 3.24 B**). The full scan ESI-MS/MS spectrum obtained from the CID process consisted of one fragment ion at  $m/z$  287 which were tentatively identified as cyanidin aglycone. From the full-scan ESI-MS/MS spectrum, an ion at  $m/z$  449 corresponding to the molecular ion  $[M]^+$  of cyanidin glucoside and the  $m/z$  287 corresponding to cyanidin

aglycone by the loss of a glucose unit (162 Da). According to the evidence shown in the previous report<sup>69</sup>, *O*-glycosidic linkage was assigned for this anthocyanin. Because the most characteristic fragmentation pathways of *C*-glucosyl flavonoid complexes were dehydration and cross-ring cleavage of the glucose moiety resulting in loss of 90 and 120 Da, which were not observed in the mass spectrum of this anthocyanin. The glycosylation site of this anthocyanin was identified at position 3 on the anthocyanin skeleton because no significant loss other than that of glucose moiety was found. This assumption on the determination of a glycosylation site was evident in the report of Davis and Brodbelt.<sup>69</sup> Since common anthocyanidins possess characteristic mass to charge ( $m/z$ ) ratio specific to their structures, it was thus proposed that the anthocyanin residues was cyanidin. Consequently, the black rice anthocyanin having molecular ion  $[M]^+$  of  $m/z$  449 was identified as cyanidin-3-*O*-glucoside.

Confirmation of the chemical structure of the black rice anthocyanin aglycone was accomplished by elucidating the fragmentation patterns of the full scan daughter ion mass spectrum obtained by LC-ESI-MS/MS. The product ion mass spectrum of the parent aglycone ion having  $m/z$  278 is shown in **Figure 3.25**. Various fragment ions were shown in this mass spectrum, which indicated the occurrence of many dissociation pathways. One possible pathway was likely to be initiated by the loss of  $H_2O$  followed by a series of CO yielding the major product ions of  $m/z$  269 (loss of water), 241 (loss of CO), 213 (loss of CO), 185 (loss of CO), and 157 (loss of CO). The prominent ion at  $m/z$  137 was supposed to form by the cleavage of the *C*-ring at positions 0 and 2 ( $^{0,2}B^+$  ion), whereas the cleavage of the *C*-ring at positions 0 and 3,

resulted in  $^{0,3}A^+$  ion at  $m/z$  121. Thus, cyanidin-3-*O*-glucoside was identified as one of the major anthocyanins found in bran of Khumdoisakhet of rice cultivars.

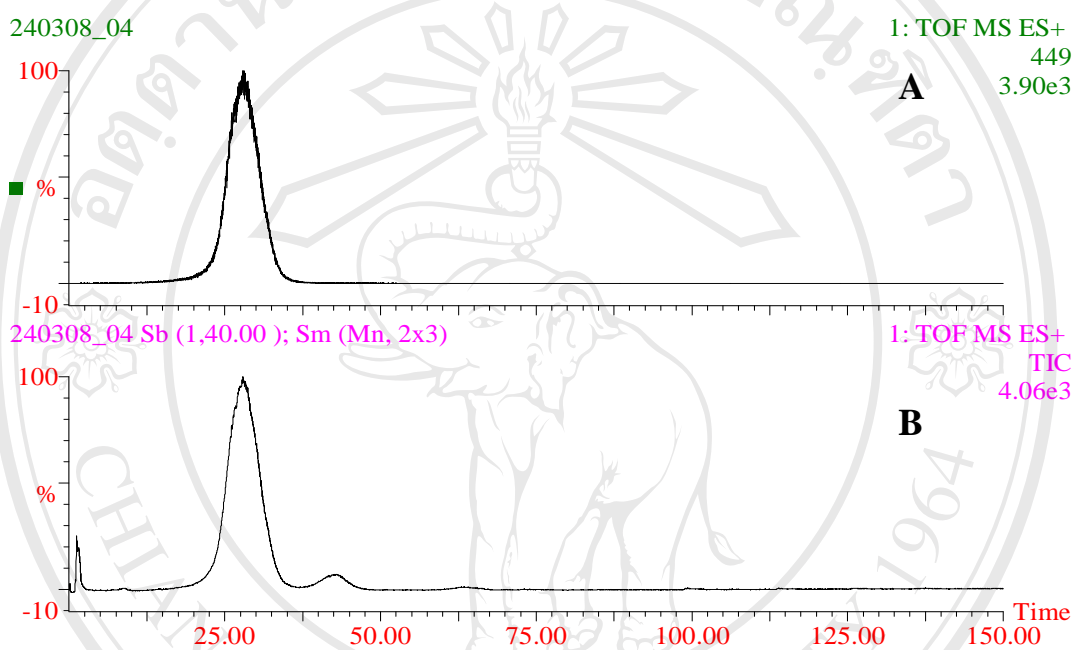


**Figure 3.23** Chromatograms obtained from LC-ESI-MS of an extract from bran of the black rice cultivar Khumdoisakhet; (A) Mass chromatogram of  $m/z$  449 (B) Total ion chromatogram.



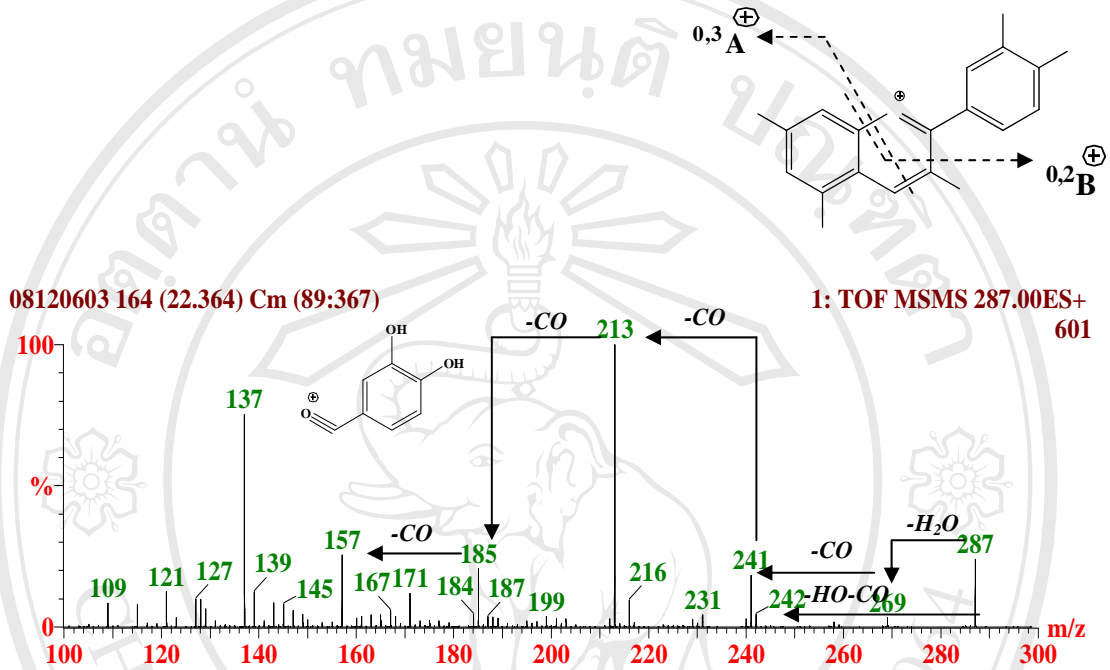


**Figure 3.25** MS/MS spectra of the parent ion at  $m/z$  287 obtained by LC-ESI-MS/MS of the extract from leaves of the black rice cultivar Khumdoisakhet showing fragmentation pathways of some ions as well as the neutral losses.

### Peonidin-3-*O*-glucoside

The TIC and mass chromatogram of  $m/z$  463 obtained from LC-ESI-MS of the extracts from bran and seed of the black rice cultivar Khumdoisakhet are shown in **Figure 3.26**. The molecular ion at  $m/z$  463 was detected at retention time 42.76 min as shown in the mass chromatogram. Full scan ESI-MS spectrum obtained from LC-ESI-MS of the bran of the black rice extract shown in **Figure 3.27 A** indicated the molecular ion  $[M]^+$  of peonidin glucoside (MW 463). The parent ion at  $m/z$  463 was selected as a precursor ion for CID operation by argon gas in order to achieve the MS/MS spectrum which gave the dissociation pattern of peonidin glucoside (**Figure 3.27B**). The full scan ESI-MS/MS spectrum of the parent ion at  $m/z$  463 obtained from the CID process consisted of only one fragment ion at  $m/z$  301 which was tentatively identified as peonidin aglycone.

An ion at  $m/z$  463 in the full-scan ESI-MS/MS corresponding to the molecular ion  $[M]^+$  of peonidin glucoside and  $m/z$  301 corresponding to peonidin aglycone by the loss of a glucose unit (162 Da). The glycosylation site of this anthocyanin was identified at position 3 with the *O*-glycosidic linkage on the anthocyanin skeleton because no significant loss other than that of glucose moiety was found. This assumption on the determination of a glycosylation site was stated in the previous section. Since common anthocyanidins possess characteristic mass to charge ( $m/z$ ) ratio specific to their structures, it was thus proposed that the anthocyanin residue was cyanidin. Consequently, the black rice anthocyanins having molecular ion  $[M]^+$  of  $m/z$  463 was identified to be peonidin-3-*O*-glucoside.

Confirmation of the chemical structure of the black rice anthocyanin aglycone was accomplished by elucidating the fragmentation pattern of the full scan daughter ion mass spectrum obtained by LC-ESI-MS/MS. The product ion mass spectrum of the parent aglycone ion having  $m/z$  301  $[M]^+$  is shown in **Figure 3.28**. It was interesting to note that some low molecular weight daughter ions produced by cleavages of the aglycone ring were not present in this mass spectrum. This could be a consequence of the stability of the base peak at  $m/z$  286, an ion resulting from a loss of  $CH_3$  radical. The subsequent fragmentation by losses of the CO neutral molecules along with  $[H+CO]^+$  radical yielded a series of ion of  $m/z$  257, 258, 229, 230, 202, and 201. Thus, peonidin-3-*O*-glucoside was identified as one of the major anthocyanins in bran of Khumdoisakhetrice cultivars.

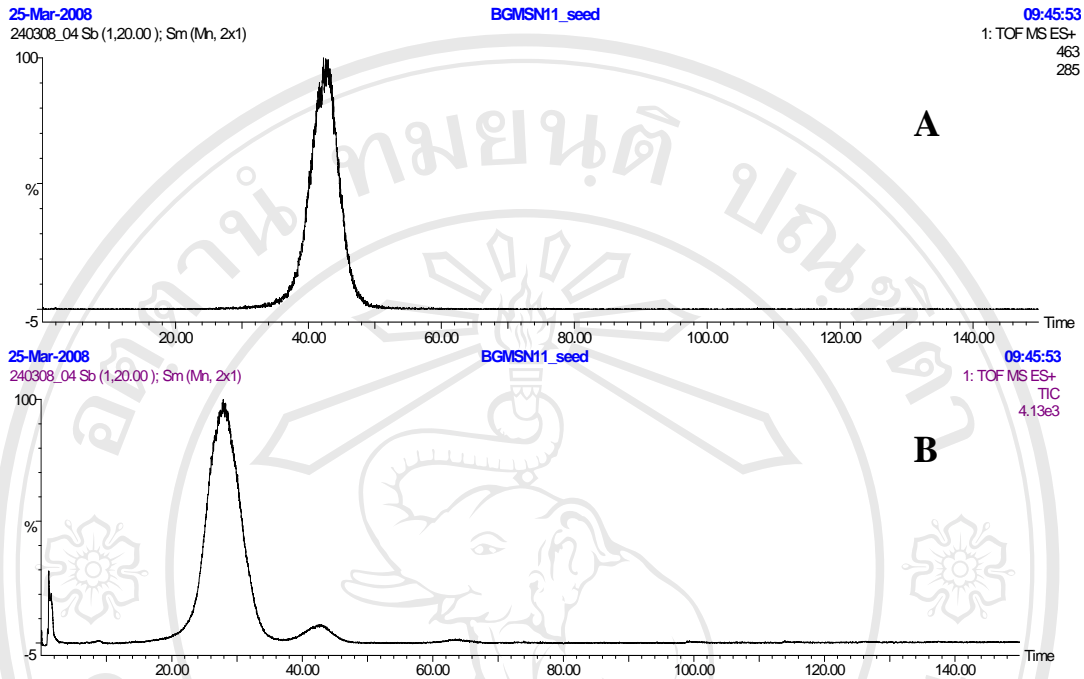


**Figure 3.26** Chromatograms obtained from LC-ESI-MS of an extract from bran of the black rice cultivar BGMSN 11; (A) Mass chromatogram of  $m/z$  463 (B) Total ion chromatogram.



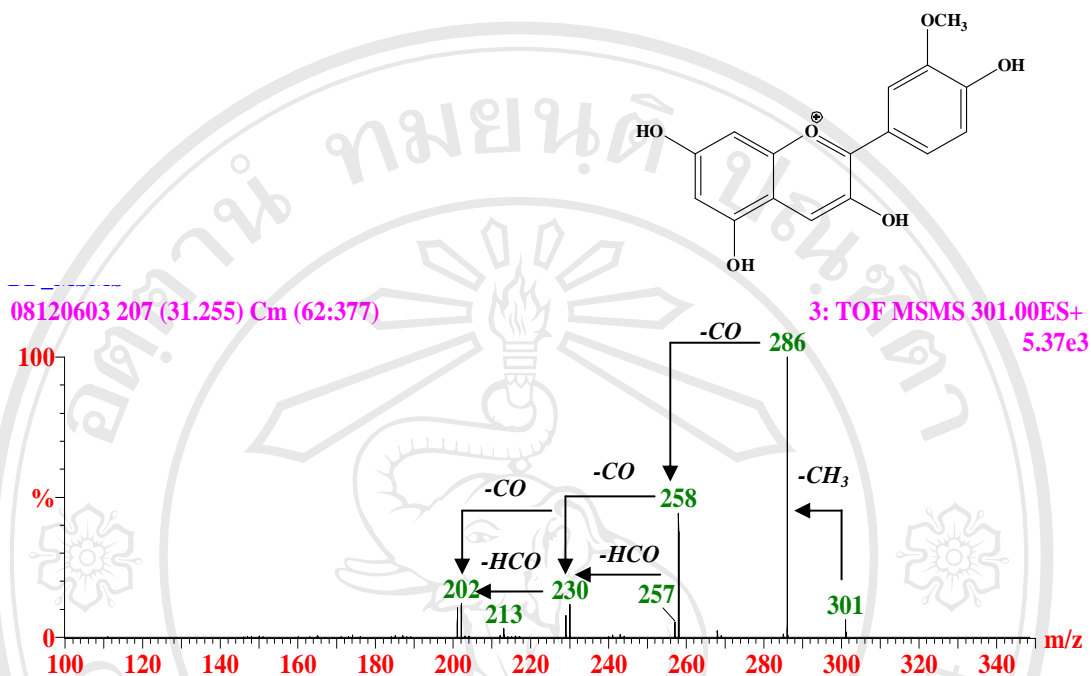


**Figure 3.28** ESI-MS/MS spectra of the parent ion at  $m/z$  301 obtained by LC-ESI-MS/MS of the extract from leaves of the black rice cultivar Khumdoisakhet showing fragmentation pathways of some ions as well the neutral losses.

### 3.3.3.5 Anthocyanins in leaves of the Thai black rice

Structures of the black rice leaf anthocyanins were identified or characterized using the data obtained from UV-Vis spectra, full scan mass spectra obtained by ESI-MS and MS/MS spectra of the suspect anthocyanin component of the black rice leaf sample extracts in the same manner as described in the previous section. Apart from cyanidin-3-*O*-glucoside the additional anthocyanins found are as follows:

### Cyanidin-3-*O*-glucoside-5-*O*-rhamnoside

The TIC and mass chromatogram of  $m/z$  595 obtained from LC-ESI-MS of the extract from leaves of the black rice cultivar Khumdoisakhet are shown in **Figure 3.29**. The molecular ion at  $m/z$  595 was detected at retention time 38.83 min as shown in the mass chromatograms. Full scan ESI-MS indicated the molecular ion of cyanidin glucoside rhamnoside (MW 595). The parent ion at  $m/z$  595 was selected as a precursor ion for CID operation in order to achieve the ESI-MS/MS spectrum, which gave the dissociation of cyanidin glucoside rhamnoside (**Figure 3.30 B**). The full scan ESI-MS/MS spectrum of the parent ion at  $m/z$  595 obtained from the CID process in the LC-MS/MS consisted of the two fragment ions at  $m/z$  287 and 449, which were cyanidin aglycone and cyanidin glucoside, respectively.

From the full-scan ESI-MS/MS spectrum, an ion of  $m/z$  595 corresponded to the molecular ion of cyanidin glucoside rhamnoside. The fragment ion of  $m/z$  449 and 287 were resulted from the loss of a rhamnose unit (146 Da) followed by a glucose unit (162 Da), respectively. The fragment ion at  $m/z$  287 indicated that the aglycone of this anthocyanin was cyanidin. The glycosylation sites of this anthocyanins were identified at position 3 and 5 on the anthocyanin skeleton because the fragmentation of the molecular ion led to the formation of three fragment ions, one corresponding to the aglycone, another corresponding to the 3-*O*-glucoside and the last to the 5-*O*-rhamnoside and no significant loss other than those of glucose and rhamnose moiety was found. This anthocyanin was thus identified as cyanidin-3-*O*-glucoside-5-*O*-rhamnoside.

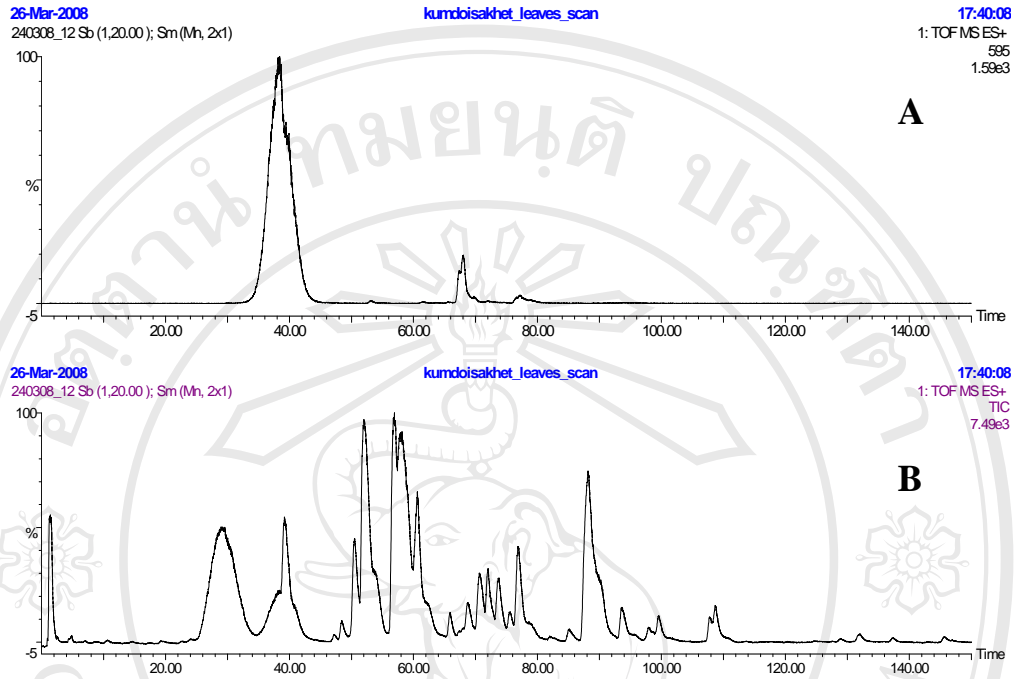


**Figure 3.29** Chromatograms obtained from LC-ESI-MS of an extract from leaves of the black rice cultivar Khumdoisakhet; (A) Mass chromatogram of  $m/z$  595 (B) Total ion chromatogram.



### **Cyanidin-3-*O*-diglucoside-5-*O*-glucoside**

The TIC and mass chromatogram of  $m/z$  773 obtained from LC-ESI-MS of the extract from leaves of the black rice cultivar Khumdoisakheth are presented in **Figure 3.31**. The molecular ion  $[M]^+$  at  $m/z$  773 was detected at retention time 65.93 min as shown in the mass chromatogram. Full scan ESI-MS spectrum obtained from LC-ESI-MS of the extract shown in **Figure 3.32** indicated the molecular ion of cyanidin triglucoside (MW 773). The parent ion at  $m/z$  773 was selected as a precursor ion for CID in order to achieve the ESI-MS/MS, spectrum which gave the informative dissociation pattern of the anthocyanins (**Figure 3.32 B**). The full scan ESI-MS/MS spectrum of the parent ion at  $m/z$  773 provided only one fragment ion of  $m/z$  449, which was characterized to be a cyanidin-3-*O*-glucoside. Fragmentation of the molecular ion which resulted in the production of  $m/z$  611 corresponding to the loss of a glucose unit and  $m/z$  449 ( $Y_1^+$ ) by the loss of two glucose units (162+162 Da) indicating the anthocyanin glycoside to be cyanidin-3-*O*-glucoside. Some weak peak signals were observed at  $m/z$  431 ( $Z_1^+$ ), 329 ( $^{0,2}X_0Y_1^+$ ), 287 ( $Y_0^+$ ) and 163 ( $B_1^+$ ). Thus, this anthocyanin was identified as cyanidin-3-*O*-diglucoside-5-*O*-glucoside.

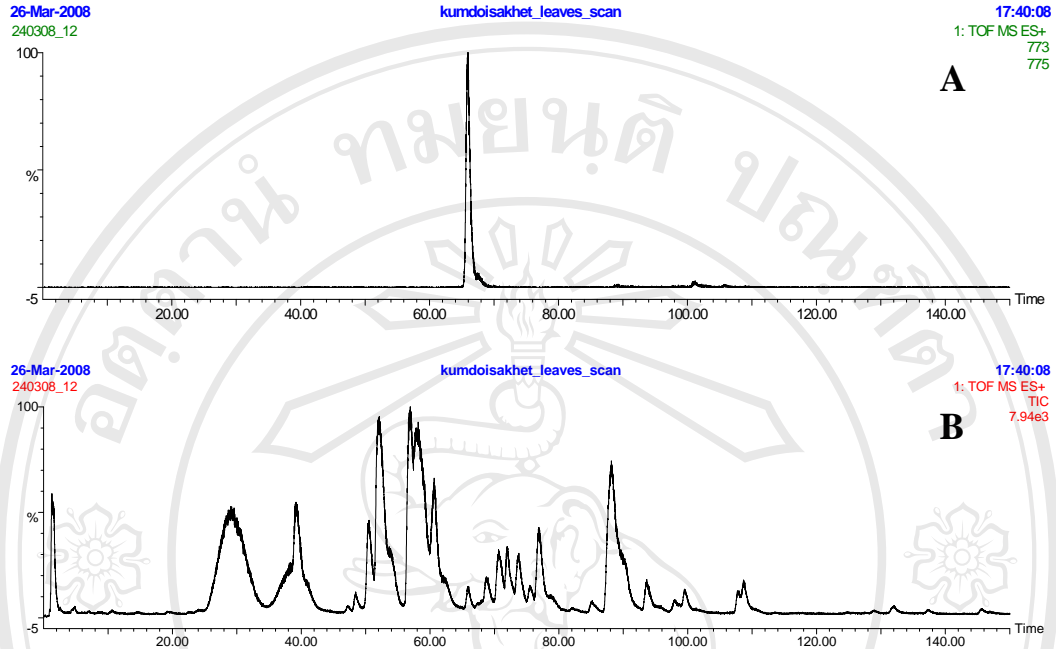


**Figure 3.31** Chromatograms obtained from LC-ESI-MS of an extract from leaves of the black rice cultivar Khumdoisakhet; (A) Mass chromatogram of  $m/z$  773 (B) Total ion chromatogram.



### Cyanidin-3-*O*-xyloside glucoside

The TIC and mass chromatogram of  $m/z$  581 obtained from LC-ESI-MS of the extract from leaves of the black rice cultivar Khumdoisakhet are shown in **Figure 3.33**. The molecular ion  $[M]^+$  at  $m/z$  581 was detected at retention time 50.25 min as shown in the mass chromatogram. This molecular ion had mass equal to that of cyanidin-3-*O*-xyloside glucoside. It was then selected as a precursor ion for CID operation using argon as collision gas. Full-scan ESI-MS/MS spectrum of the parent ion at  $m/z$  581 gave product ion at  $m/z$  443, 497, 516, 524, 545, and 563 corresponding to the loss of a series of water ( $m/z$  18). The ion at  $m/z$  287 was the cyanidin aglycone. Thus, this anthocyanin was identified as cyanidin-3-*O*-xyloside glucoside.

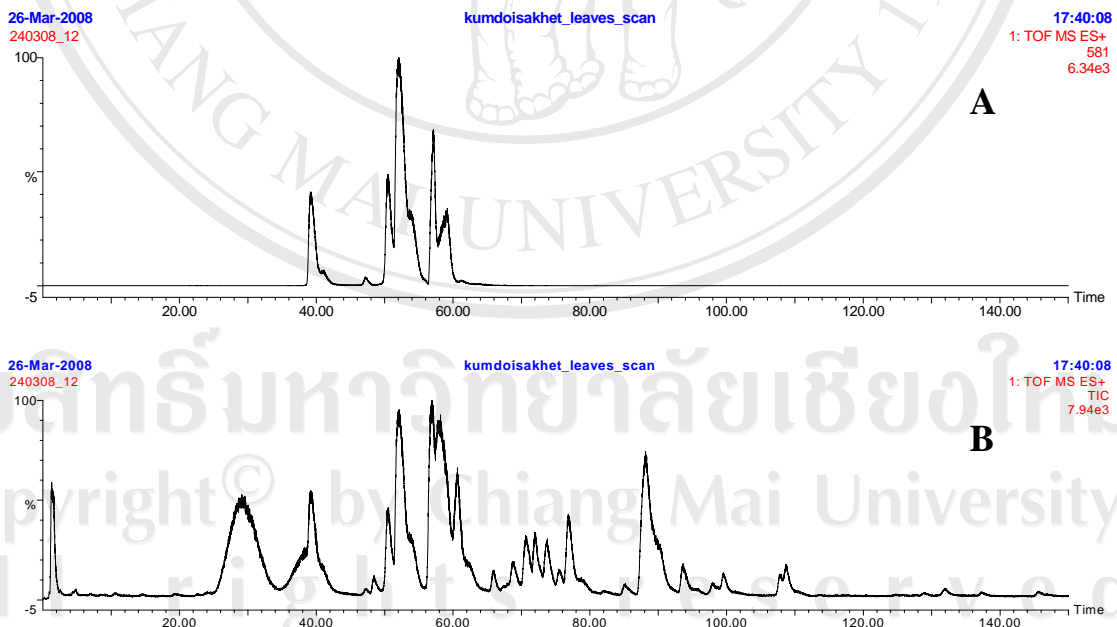


**Figure 3.33** Chromatograms obtained from LC-ESI-MS of an extracts from leaves of the black rice cultivar Khumdoisakhet; (A) Mass chromatogram of  $m/z$  581 (B) Total ion chromatogram.



### Cyanidin-3-*O*-xyloside glucoside (isomer)

TIC and mass chromatogram of the ion at  $m/z$  581 obtained from LC-ESI-MS of the extract from leaves of the black rice cultivars, Khumdoisakhet are shown in **Figure 3.35**. The molecular ion at  $m/z$  581 was detected at retention time 53.26 min as shown in the mass chromatogram. Full scan ESI-MS spectrum obtained from LC-ESI-MS of the extract shown in **Figure 3.36** indicated the molecular ion of cyanidin-3-*O*-xyloside glucoside (MW 581), the same as that of the previous component at retention time 50.25 min. This parent ion at  $m/z$  581 was selected as a precursor ion for CID operation by argon gas in order to achieve the ESI-MS/MS spectrum which gave the dissociation pattern similar to the anthocyanin identified before. The full scan ESI-MS/MS spectrum at  $m/z$  581 presented the base peak at  $m/z$  563 and other mass ions of  $m/z$  545, 527, 516, 473, 461 and 433. The full-scan ESI-MS/MS spectrum of product ions of the at  $m/z$  581 (**Figure 3.36**) shows ions at  $m/z$  563  $[M-H_2O]^+$ , 545  $[M-2H_2O]^+$ , 527  $[M-3H_2O]^+$ , 515, 473, 461 and 433 corresponding to loss of series of water ( $m/z$  18), and the  $m/z$  287 indicating that the aglycone of this anthocyanins was cyanidin. Thus, this anthocyanin was identified as an isomer cyanidin-3-*O*-xyloside glucoside. Structural difference between these two isomers of cyanidin-3-*O*-xyloside glucoside is expected to be due to the position of O-glycoside linkage.

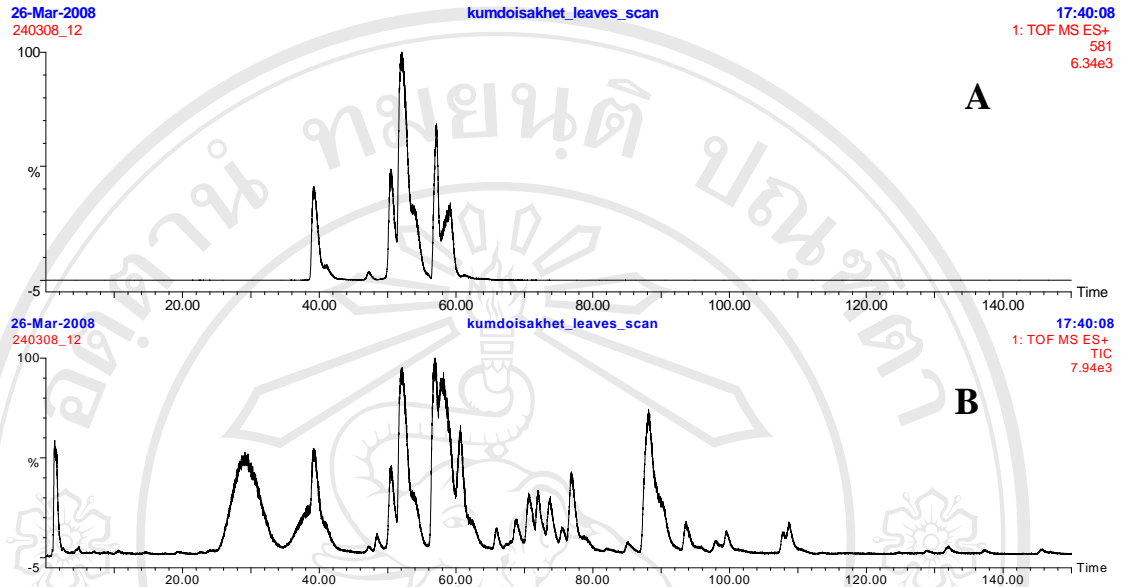


**Figure 3.35** Chromatograms obtained from LC-ESI-MS of an extract from leaves of the black rice cultivar Khumdoisakhet; (A) Mass chromatogram of  $m/z$  581(B) Total ion chromatograms.

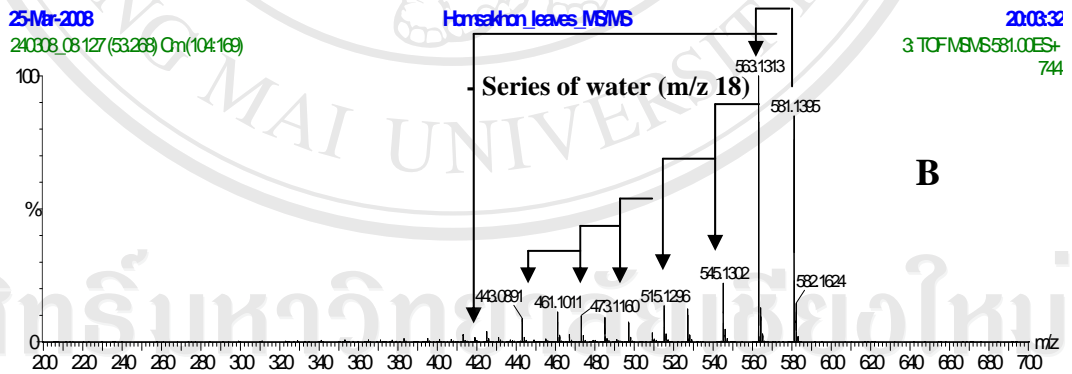
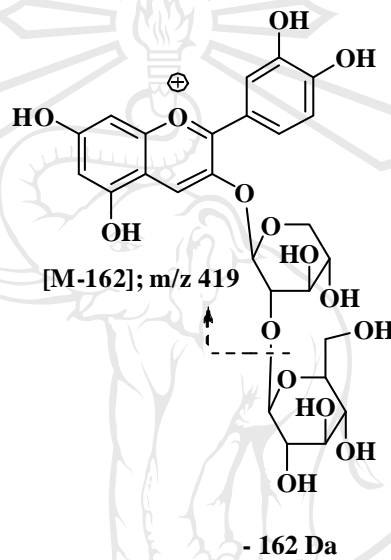
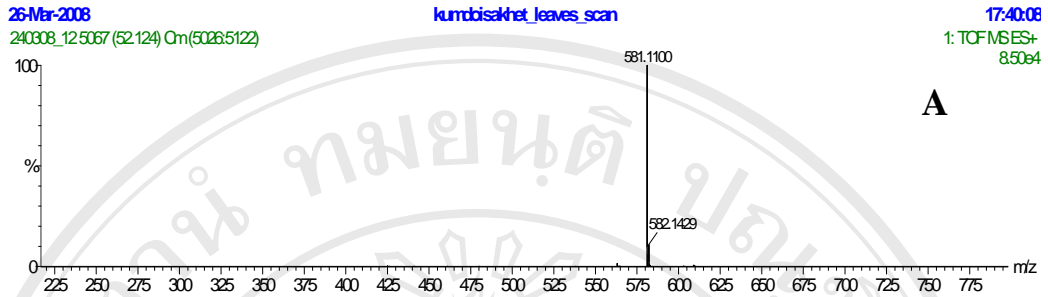


**Figure 3.36** Full scan mass spectra of an extracts from the black rice cultivar, Khumdoisakhet obtained by; (A) ESI-MS (B) ESI-MS/MS.

### Cyanidin-3-*O*-diglucoside

The TIC and mass chromatogram of  $m/z$  611 obtained from LC-ESI-MS of the extract from leaves rice cultivar Khumdoisakheat are shown in **Figure 3.37**. The molecular ion  $[M]^+$  at  $m/z$  611 was detected at retention time 56.92 min as shown in the mass chromatogram. This molecular ion had mass equal to that of cyanidin diglucoside. It was then selected as a precursor ion for CID operation by argon gas in order to achieve the ESI-MS/MS spectrum, which gave the dissociation pattern useful for structural identification. The full scan ESI-MS/MS spectrum of the parent ion at  $m/z$  611 provided fragment ions at  $m/z$  287, 329, 431, and 449. The ion at  $m/z$  611 corresponding to the molecular ion of cyanidin diglucoside. Relatively abundance Y type ions were observed at  $m/z$  287 ( $Y_0^+$ ) corresponding to cyanidin aglycone and  $m/z$  449 ( $Y_1^+$ ) corresponding to cyanidin-3-*O*-glucoside. Other ions at  $m/z$  431 ( $Z_1^+$ ), and 329 ( $^{0,2}X_0Y_1^+$ ) formed by common fragmentation routes were also present.  $^{0,2}X_0^{0,2}X_1^+$  and  $^{0,2}X_0Y_1^+$  ions can be considered as characteristic of the 1-2 interglycosidic linkage in 3-*O*-glycoside adducts. Additional fragment ions at  $m/z$  413 [ $Y_1^+-2H_2O$ ], and 353 [ $Y_1^+-2H_2O-60$ ] were also observed. The formation of  $Z_1^+$  ( $m/z$  431) ion is useful for establishing that the eliminated terminal carbohydrate unite is linked to another carbohydrate and not directly to the aglycone and could be of analytical value for the differentiation of *O*-diglucosyl and di-*O*-glucosyl anthocyanins. In addition the *O*-glycosidic linkage was assigned as (1-6) because of the higher intensity of the  $Y_1^+$  ( $m/z$  449) ion compared to that of the  $Y_0^+$  ( $m/z$  287) ion. Thus, this anthocyanin was identified as cyanidin-3-*O*-diglucoside.

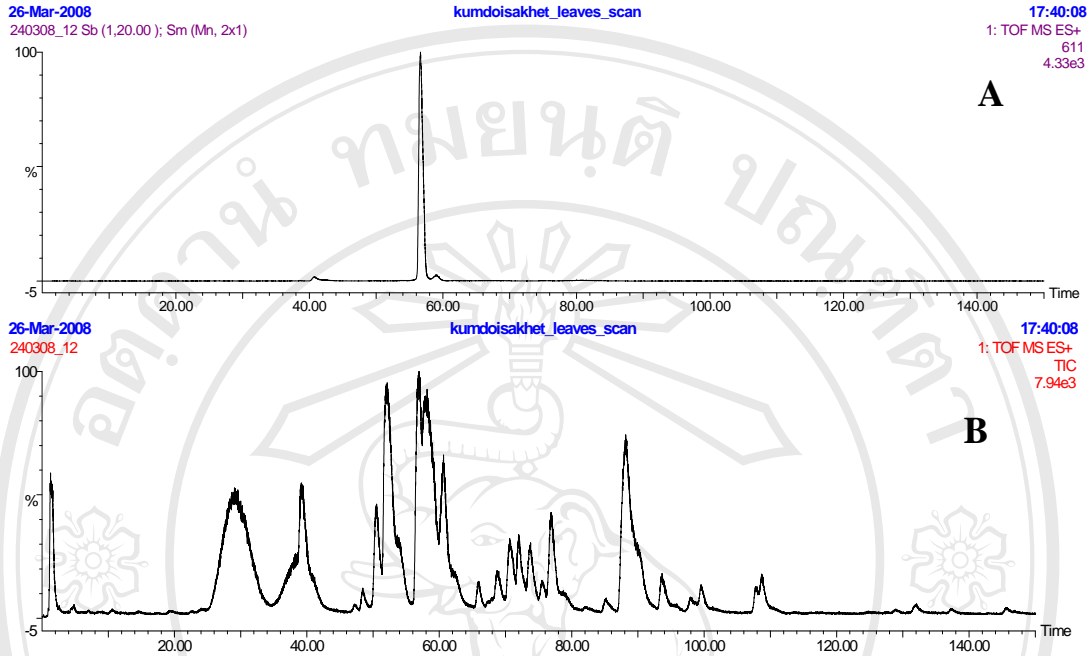


**Figure 3.37** Chromatograms obtained from LC-ESI-MS of an extract from leaves of the black rice cultivar Khumdoisakhet; (A) Mass chromatogram of  $m/z$  611 (B) Total ion chromatogram.

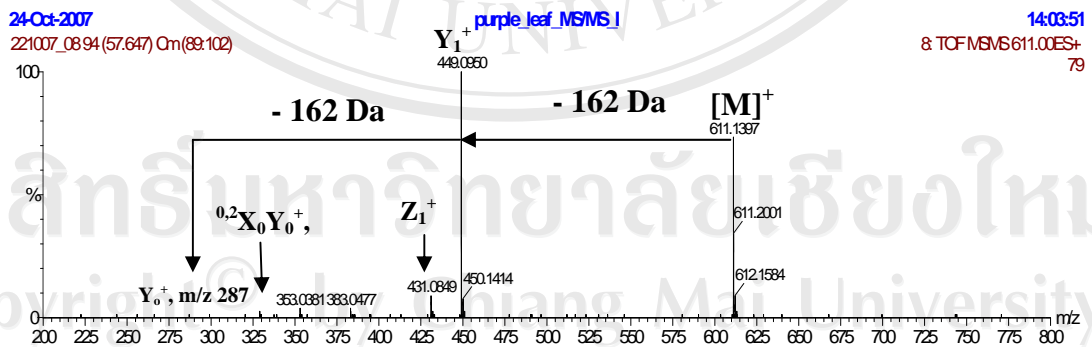
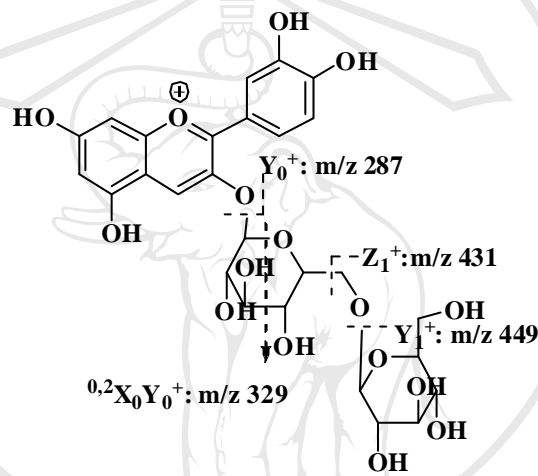
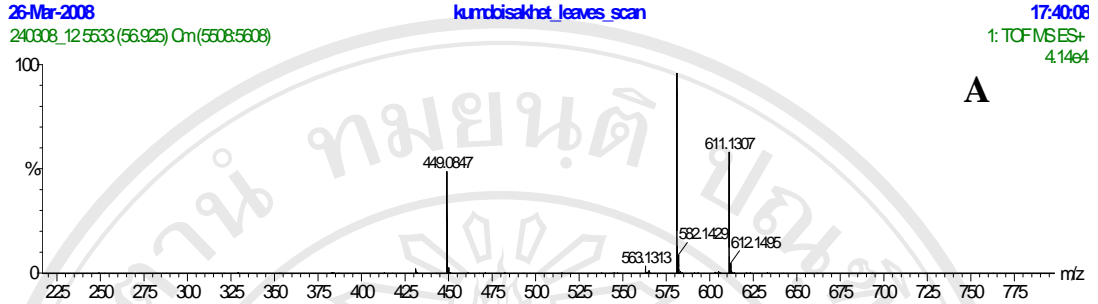


**Figure 3.38** Full scan mass spectra of an extracts from leaves of the black rice cultivar Khumdoisakhet obtained by; (A) ESI-MS (B) ESI-MS/MS.

### **Cyanidin-3-*O*-(*p*-coumaroyl)glucoside-5-*O*-glucoside**

The TIC and mass chromatogram of  $m/z$  757 obtained from LC-ESI-MS of the extracts from leaves of the black rice cultivar Khumdoisakhet are presented in **Figure 3.39**. The molecular ion  $[M]^+$  at  $m/z$  757 was detected at retention time 72.00 min as shown in the mass chromatogram. Full scan ESI-MS spectrum obtained from LC-ESI-MS of the extracts shown in **Figure 3.40** indicated the molecular ion of cyanidin with two glucose units and one coumaroyl group (MW 146). The parent ion at  $m/z$  757 was selected as a precursor ion for CID operation using argon as collision gas in order to achieve the ESI-MS/MS spectrum which would give the dissociation pattern useful for structural identification. The full scan ESI-MS/MS spectrum at  $m/z$  757 obtained from the CID process consisted of two fragment ions at  $m/z$  287 and 449, which were a cyanidin aglycone and cyanidin-3-*O*-glucoside, respectively. An ion of  $m/z$  757 corresponding to the molecular ion of this anthocyanin. The other ions at  $m/z$  449 and 287 corresponding to cyanidin-3-*O*-glucoside and cyanidin aglycone, which were derived from the losses of (*p*-coumaroyl)glucoside unit (308 Da), indicating that the adduct of the glucose unit at position 3 was a coumaroyl group (146 Da), and glucose unit (162 Da), respectively. Other ions at  $m/z$  431 ( $Z_1^+$ ), and 329 ( $^{0,2}X_0Y_1^+$ ) formed by common fragmentation routes were also present. Additional fragment ions at  $m/z$  413 [ $Y_1^+-2H_2O$ ], and 353 [ $Y_1^+-2H_2O-60$ ] were also observed. The fragmentation pattern suggested that of this anthocyanin was cyanidin-3-*O*-(*p*-coumaroyl)glucoside-5-*O*-glucoside.

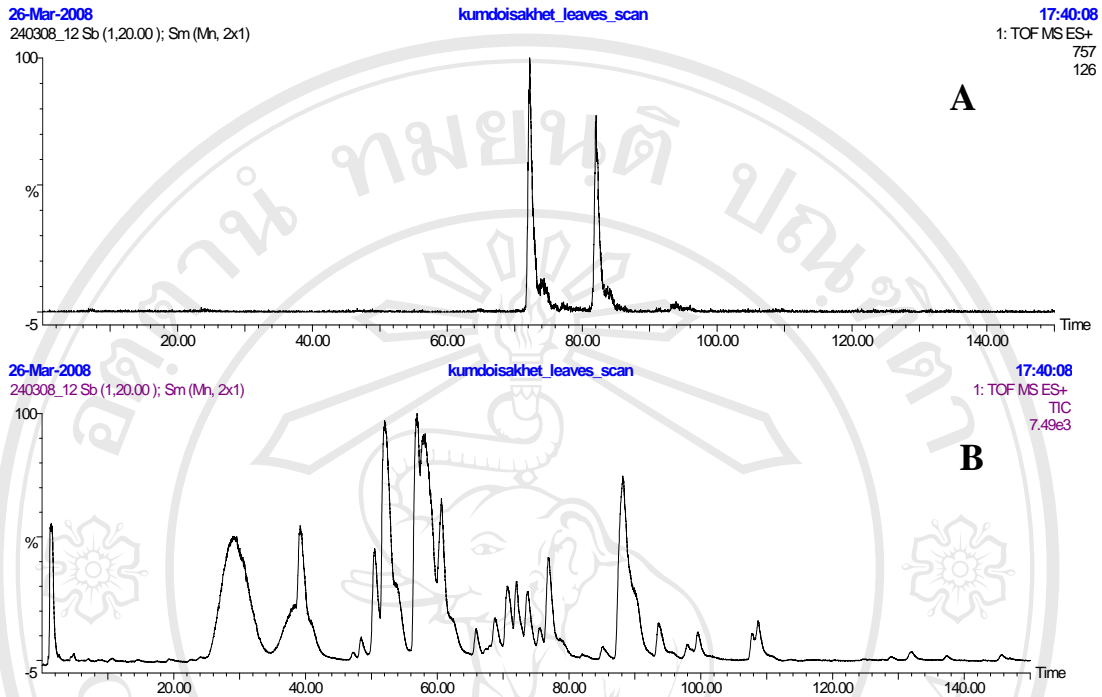


**Figure 3.40** Chromatograms obtained from LC-ESI-MS of an extract from leaves of the black rice cultivar Khumdoisakhet; (A) Mass chromatogram of  $m/z$  757 (B) Total ion chromatogram.

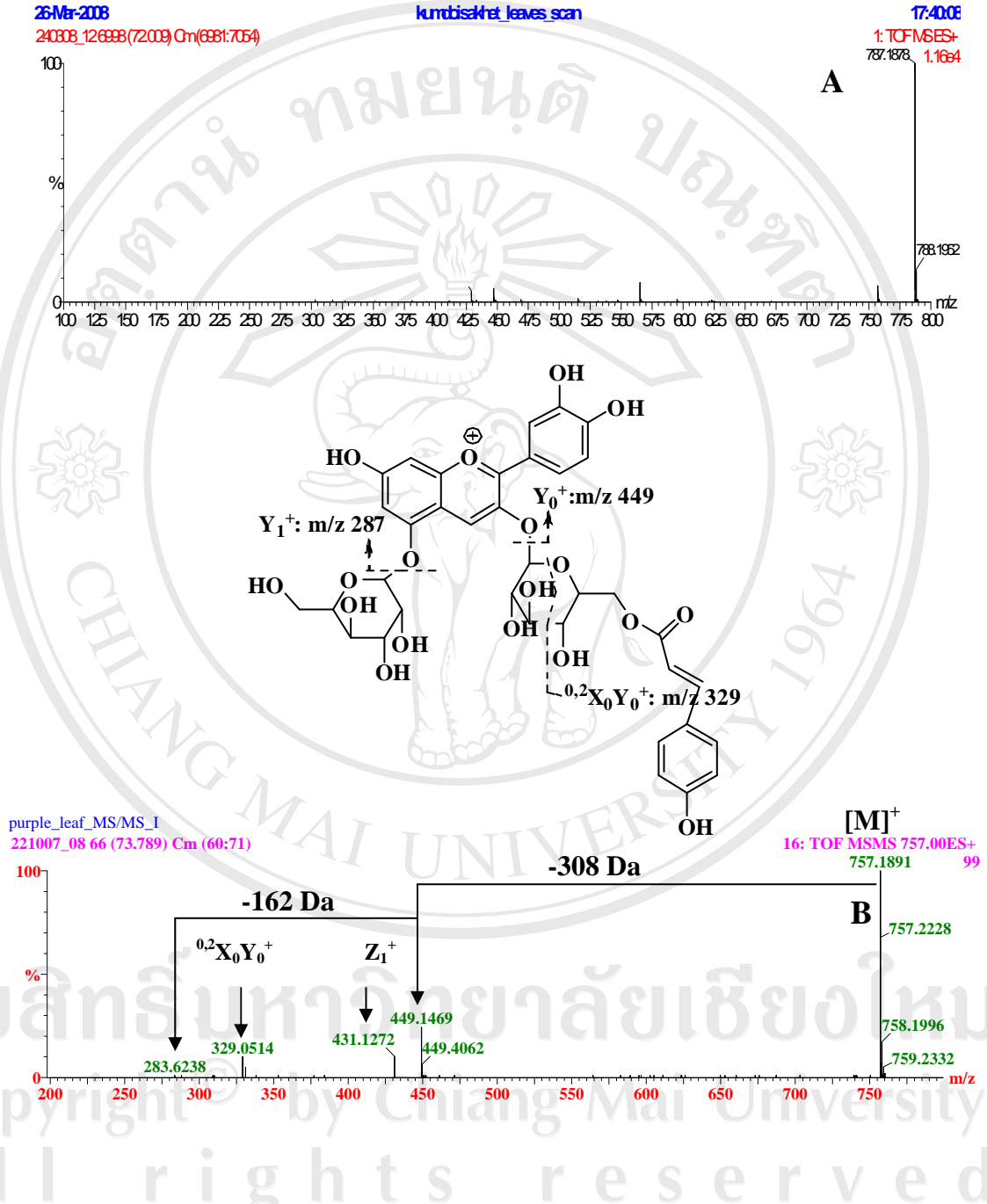


**Figure 3.40** Full scan mass spectra of an extract from leaves of the black rice cultivar

Khumdoisakhet obtained by; (A) ESI-MS (B) ESI-MS/MS.

### **Cyanidin-3-*O*-(feruloyl)glucoside-5-*O*-glucoside**

The TIC and mass chromatogram of  $m/z$  787 obtained from LC-ESI-MS of the extract from leaves of the black rice cultivar Khumdoisakhet are shown in **Figure 3.41**. The molecular ion at  $m/z$  787 was detected at retention time 72.20 min as shown in the mass chromatogram. The full scan ESI-MS spectrum obtained from LC-ESI-MS of the extract shown in **Figure 3.42 A** contains a molecular ion at  $m/z$  787 of cyanidin feruloly diglucoside (MW 787). The parent ion at  $m/z$  787 was then selected as a precursor ion for CID operation using argon as collision gas and the MS/MS spectrum was achieved, which contained the fragment ions at  $m/z$  177, 287, 329, 431, 449, and 625. Fragmentation of the molecular ion which resulted in the product ions of  $m/z$  287, and 449, were corresponding to the losses of (feruloyl)glucoside unit (308 Da), and glucose unit (162 Da), respectively. Relative abundant Y type ions were observed at  $m/z$  287 ( $Y_0^+$ ) and 449 ( $Y_1^+$ ), whereas  $m/z$  431 ( $Z_1^+$ ), and 329 ( $^{0,2}X_0^+Y_1^+$ ) formed by common fragmentation routes are also present. The other fragment ions at  $m/z$  415 [ $Y_1^+ - 2H_2O$ ] $^+$ , 397 [ $Y_1^+ - 3H_2O$ ] $^+$ , and 355 [ $Y_1^+ - 2H_2O - 60$ ] $^+$ , the characteristics of anthocyanin-*O*-diglucoside, were also observed. Additional fragment ion at  $m/z$  177 indicating the presence of a feruloyl group was detected. Thus, this anthocyanin was identified as cyanidin-3-*O*-(feruloyl)glucoside-5-*O*-glucoside.

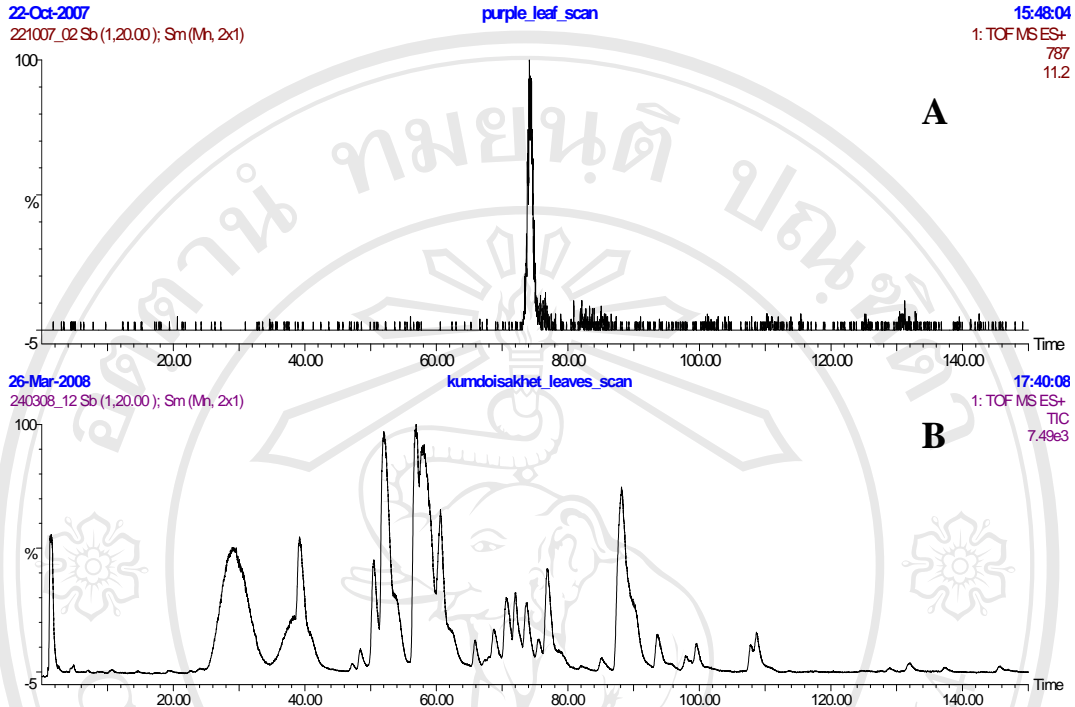


**Figure 3.41** Chromatograms obtained from LC-ESI-MS of an extract from leaves of the black rice cultivar Khumdoisakhet; (A) Mass chromatogram of  $m/z$  787 (B) Total ion chromatogram.

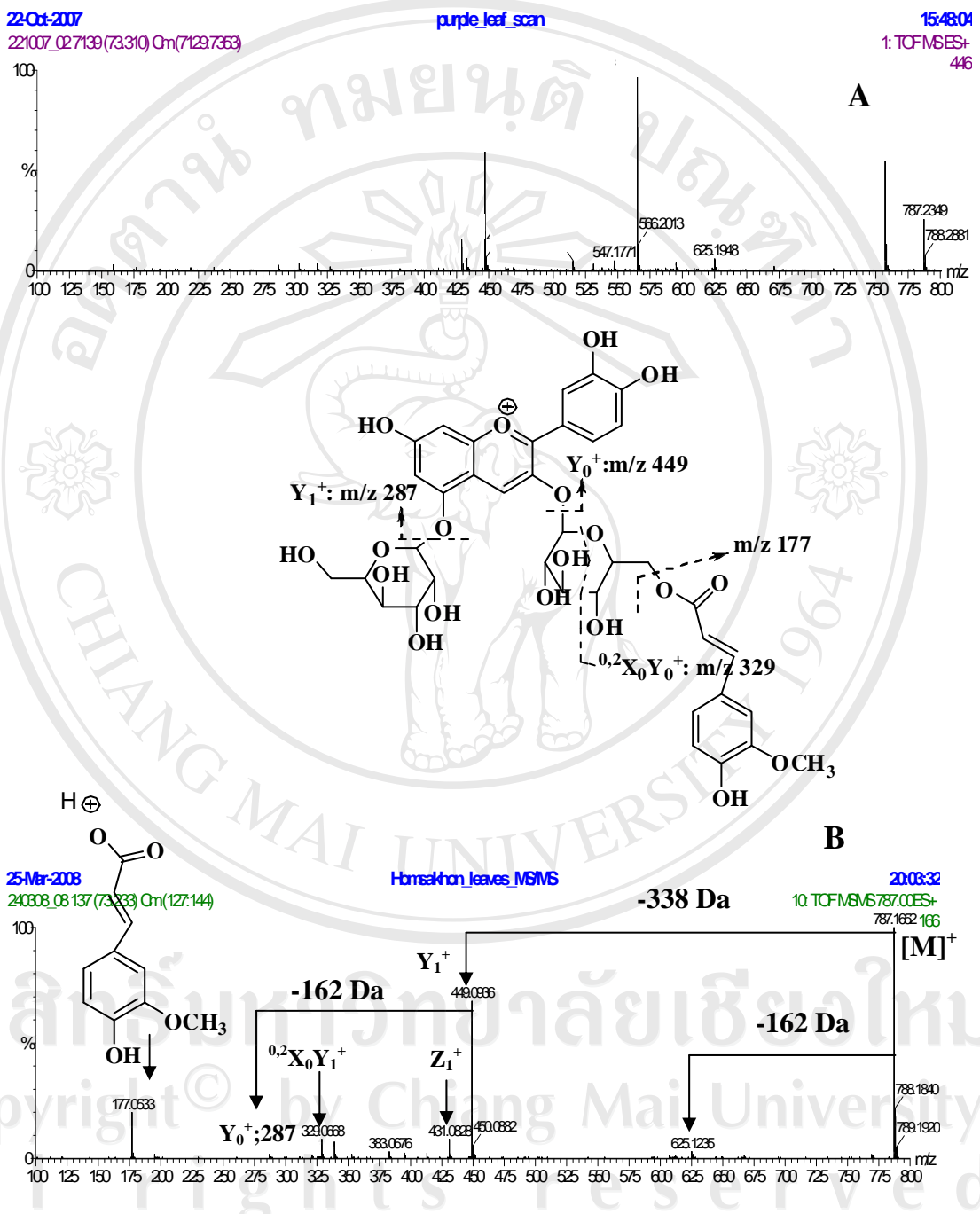


**Figure 3.42** Full scan mass spectrum of an extract from leaves of the black rice cultivar, Khumdoisakhet obtained by; (A) ESI-MS (B) ESI-MS/MS.

### Peonidin-3-*O*-diglucoside

The TIC and mass chromatogram of  $m/z$  625 obtained from LC-ESI-MS of the extract from leaves of the black rice cultivars Khumdoisakhet are shown in **Figure 3.43**. The molecular ion  $[M]^+$  at  $m/z$  625 was detected at retention time 75.02 min as shown in the mass chromatogram. Full scan ESI-MS spectrum obtained from LC-ESI-MS of the extracts shown in **Figure 3.44 A** indicated the molecular ion of peonidin diglucoside. The parent ion at  $m/z$  625 was selected as a precursor ion for CID operation using argon as collision gas in order to achieve the ESI-MS/MS spectrum. The full scan ESI-MS/MS spectrum of the parent ion at  $m/z$  625 provided various fragment ions at  $m/z$  301, 427, 445, and 463. An ion of  $m/z$  625 was assigned to the molecular ion of peonidin diglucoside. Relatively low abundance Y type ion observed at  $m/z$  301 ( $Y_0^+$ ) was corresponding to the peonidin aglycone and the high abundance ion at  $m/z$  463 ( $Y_1^+$ ) corresponding to peonidin-3-*O*-glucosie, whereas other ions at  $m/z$  445 ( $Z_1^+$ ), and 343 ( $^{0,2}X_0Y_1^+$ ) formed by common fragmentation routes were also present.  $^{0,2}X_0Y_1^+$  ions can be considered as characteristic of the 1-2 interglycosidic linkage in 3-*O*-glycoside adducts. Additional fragment ions at  $m/z$  427 [ $Y_1^+-2H_2O$ ], 397 [ $Y_1^+-2H_2O-30$ ] and 367 [ $Y_1^+-2H_2O-60$ ] were also observed. The formation of  $Z_1^+$  ( $m/z$  445) ion is useful for establishing that the eliminated terminal carbohydrate unite is linked to another carbohydrate and not directly to the aglycone and could be useful for the differentiation of *O*-diglucosyl and di-*O*-glucosyl flavonoids. In addition the *O*-diglycosidic linkage was assigned as (1-6) because of the higher intensity of the  $Y_1^+$  ( $m/z$  463) ion compared to that of the  $Y_0^+$  ( $m/z$  301) ion. Peonidin-3-*O*-

diglucoside was thus identified as one of anthocyanins in black rice cultivar Khumdoisakhet.

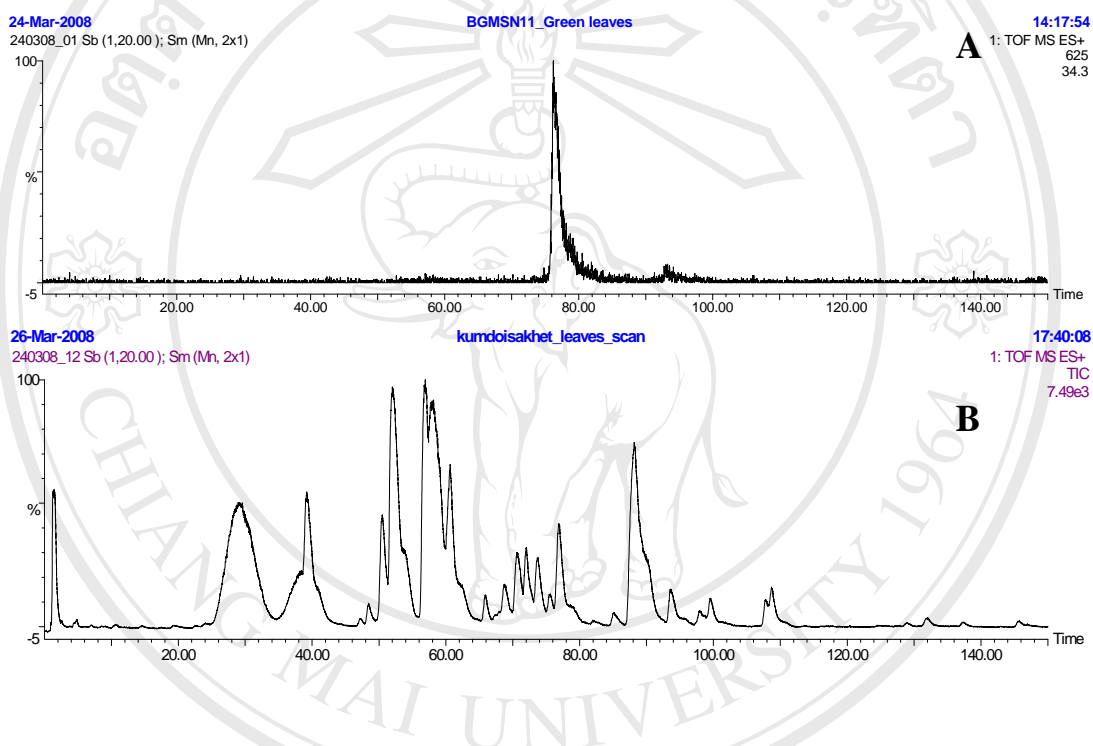


**Figure 3.43** Chromatograms obtained from LC-ESI-MS of an extract from leaves of the black rice cultivar Khumdoisakhet; (A) Mass chromatogram of  $m/z$  625 (B) Total ion chromatogram.

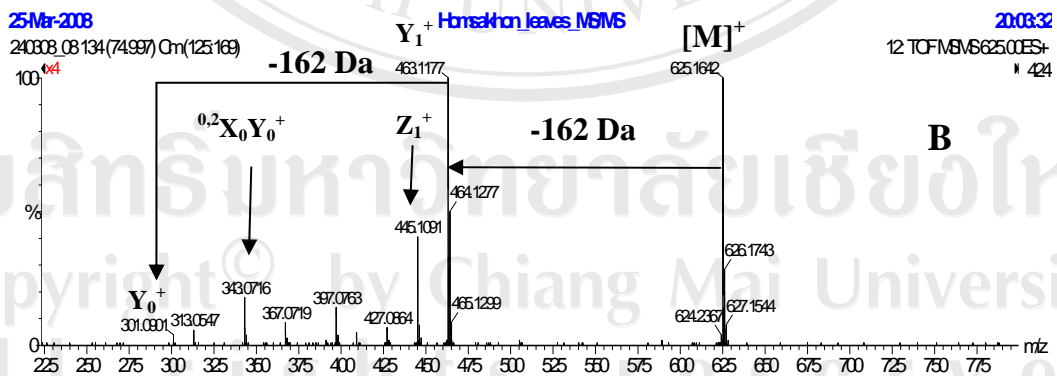
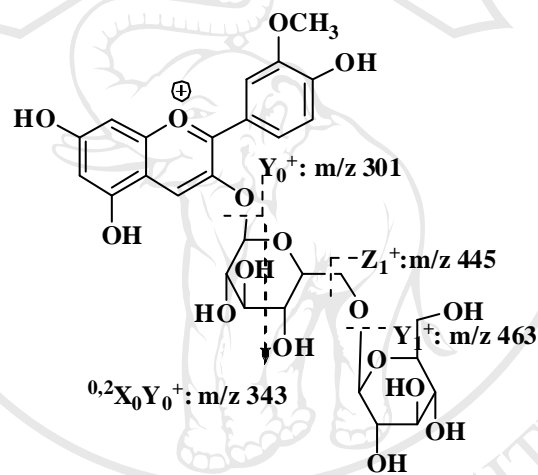
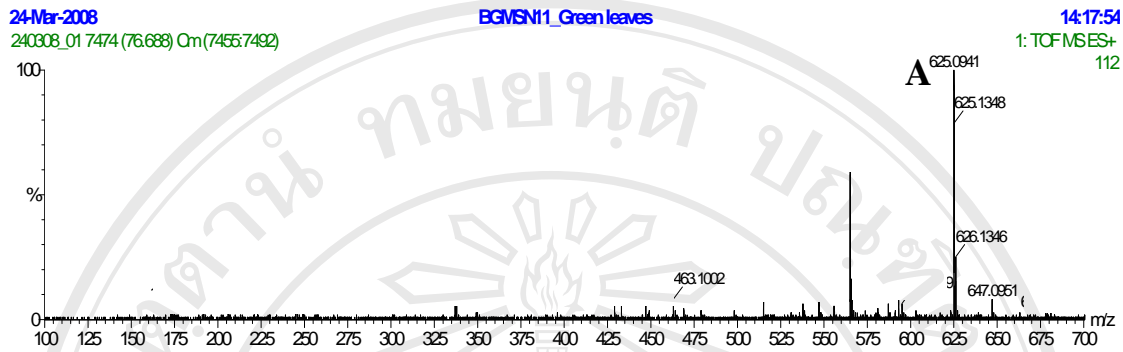


**Figure 3.44** Full scan massspectra of an extract from leaves of the black rice cultivar Khumdoisakhet obtained by; (A) ESI-MS (B) ESI-MS/MS.

**Peonidin-3-*O*-(*p*-coumaroyl)glucoside-5-*O*-xyloside**

The TIC and mass chromatogram of  $m/z$  741 obtained from LC-ESI-MS of the extract from leaves of the black rice cultivar Khumdoisakhet are shown in **Figure 3.45**. The molecular ion  $[M]^+$  at  $m/z$  741 was detected at retention time 88.91 min as shown in the mass chromatogram. Full scan ESI-MS spectrum obtained from LC-ESI-MS of the extract shown in **Figure 3.46 A** indicated the molecular ion of peonidin *O*-(*p*-coumaroyl)glucoside xyloside. The parent ion at  $m/z$  741 was selected as a precursor ion for CID operation using argon as collision gas in order to achieve the MS/MS spectrum. The full scan MS/MS spectrum of this parent ion provided various  $m/z$  301, 313, 403, 415, and 433. An ion of  $m/z$  741 was corresponding to the molecular ion of peonidin *O*-(*p*-coumaroyl)glucoside xyloside. Relatively low abundance Y type ions are observed at  $m/z$  301 ( $Y_1^+$ ) corresponding to peonidin aglycone and  $m/z$  433 ( $Y_0^+$ ) corresponding to peonidin-3-xyloside. Thus, this anthocyanin was identified as peonidin-3-*O*-(*p*-coumaroyl)glucoside-5-*O*-xyloside.

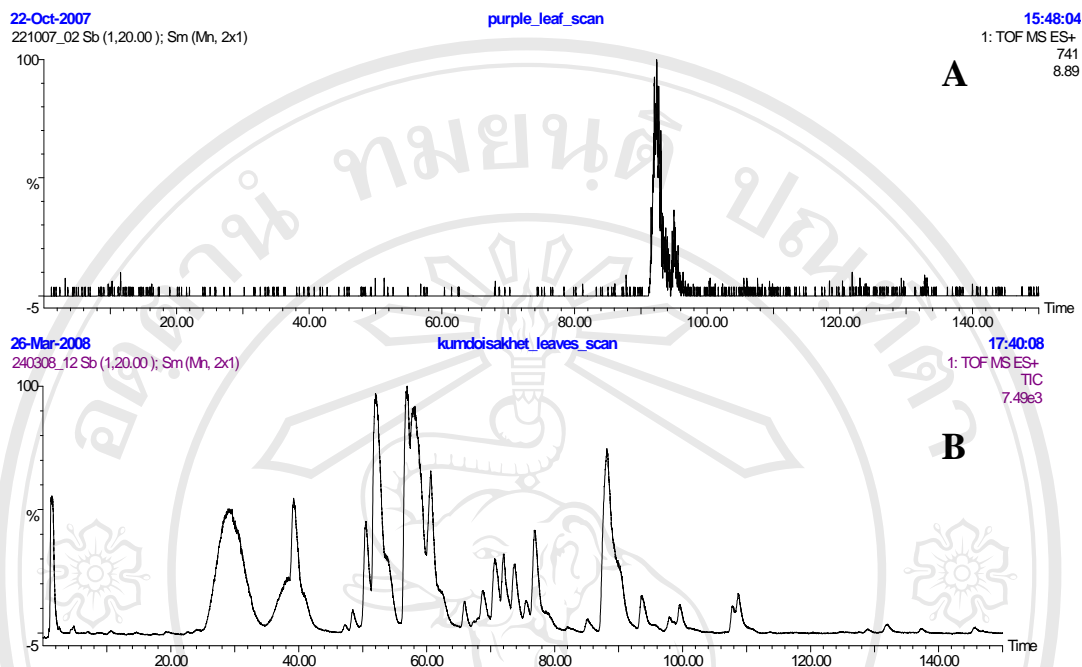


**Figure 3.45** Chromatograms obtained from LC-ESI-MS of an extract from leaves of the black rice cultivar Khumdoisakhet; (A) Mass chromatograms at  $m/z$  741 (B) Total ion chromatogram.

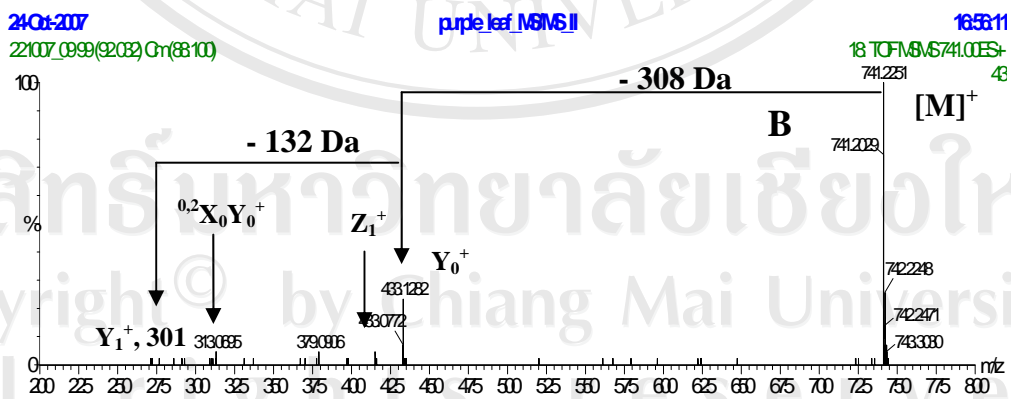
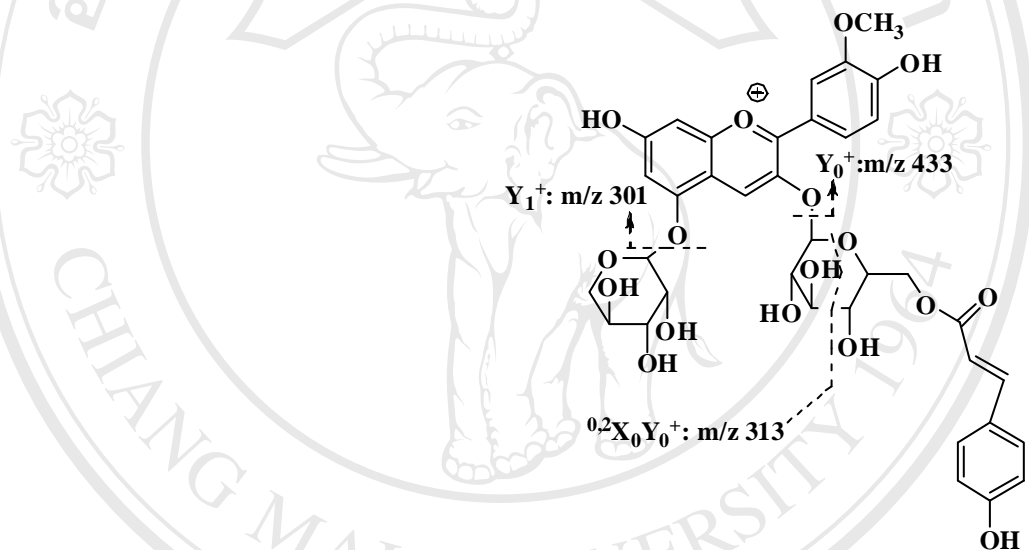
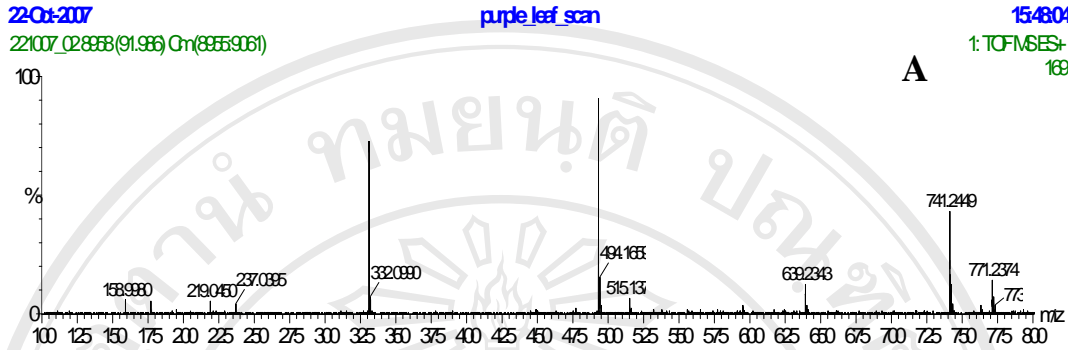


**Figure 3.57** Full scan mass spectra of an extract from leaves of the black rice cultivars, Khumdoisakhet obtained by; (A) ESI-MS (B) ESI-MS/MS.

**Mavidin-3-*O*-(*p*-coumaroyl) glucoside-5-*O*-glucoside**

The TIC and mass chromatogram of  $m/z$  801 obtained from LC-ESI-MS of the extract from the black rice cultivar Khumdoisakhet are shown in **Figure 3.47**. The molecular ion  $[M]^+$  at  $m/z$  801 was detected at retention time 89.42 min as shown in mass chromatogram. The full scan ESI-MS spectrum obtained from LC-ESI-MS of the extract shown in **Figure 3.48** indicated the molecular ion of mavidin (*p*-coumaroyl) diglucoside (MW 801). The full scan ESI-MS spectrum yielded the base peak at  $m/z$  801 and other mass ions of  $m/z$  331, and 493. Full-scan ESI-MS spectrum and fragmentation pattern presented a molecular ion  $[M]^+$  at  $m/z$  801 and the fragment ion at  $m/z$  493, and 331 which corresponds with malvidin-3-*O*-glucoside and malvidin aglycone derived from the loss of (*p*-coumaroyl)-glucoside unit (308 Da) followed by glucose unit (162 Da), respectively. Thus, this anthocyanin was identified as mavidin-3-*O*-(*p*-coumaroyl)glucoside-5-*O*-glucoside.

Confirmation of the chemical structure of the malvidin aglycone was accomplished by elucidating the fragmentation pattern of its full scan product ions obtained by LC-ESI-MS/MS. The product ion mass of the parent aglycone ion,  $[M]^+$ , having  $m/z$  331 is shown in **Figure 3.49**. The product ion mass spectrum of the malvidin aglycone ion ( $m/z$  331) showed less fragmentations and some low molecular weight daughter ions produced by cleavages of the aglycone ring were not present in this mass spectrum. This was expected to be a consequence of the stability of the fragment ion at  $m/z$  315 which was resulted from a loss of  $CH_3$  radical. The other fragment ions of the same type were at  $m/z$  287 (loss of CO) and  $m/z$  270 (loss of  $OCH_2$  radical).

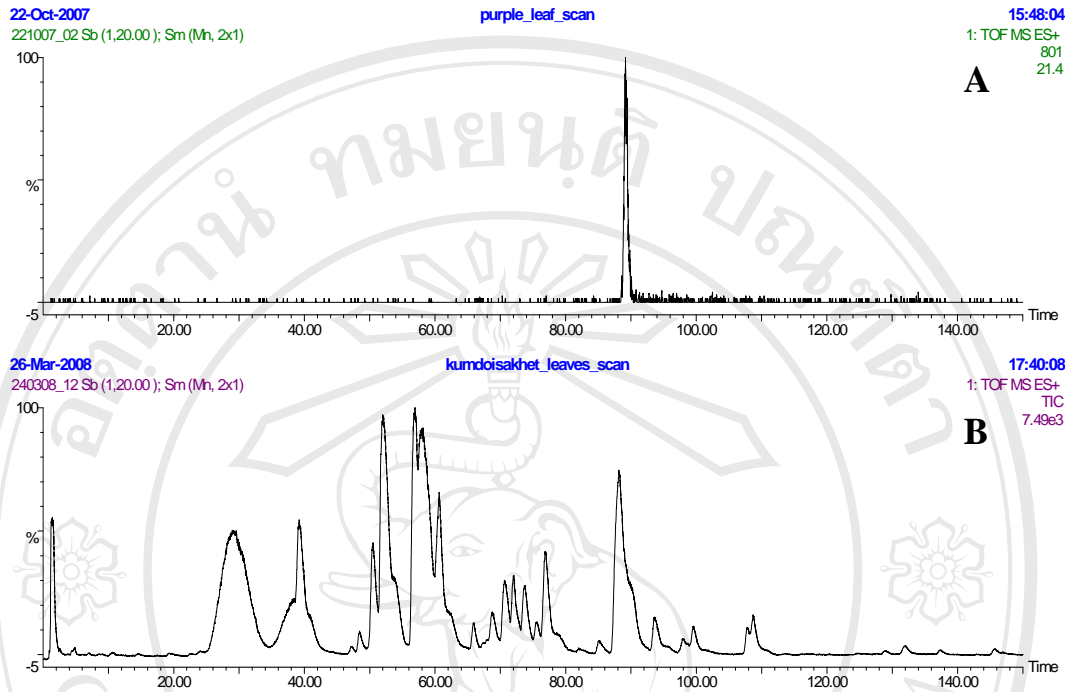


**Figure 3.47** Chromatograms obtained from LC-ESI-MS of an extract from leaves of the black rice cultivar Khumdoisakhet ; (A) Mass chromatogram of  $m/z$  801 (B) Total ion chromatogram.

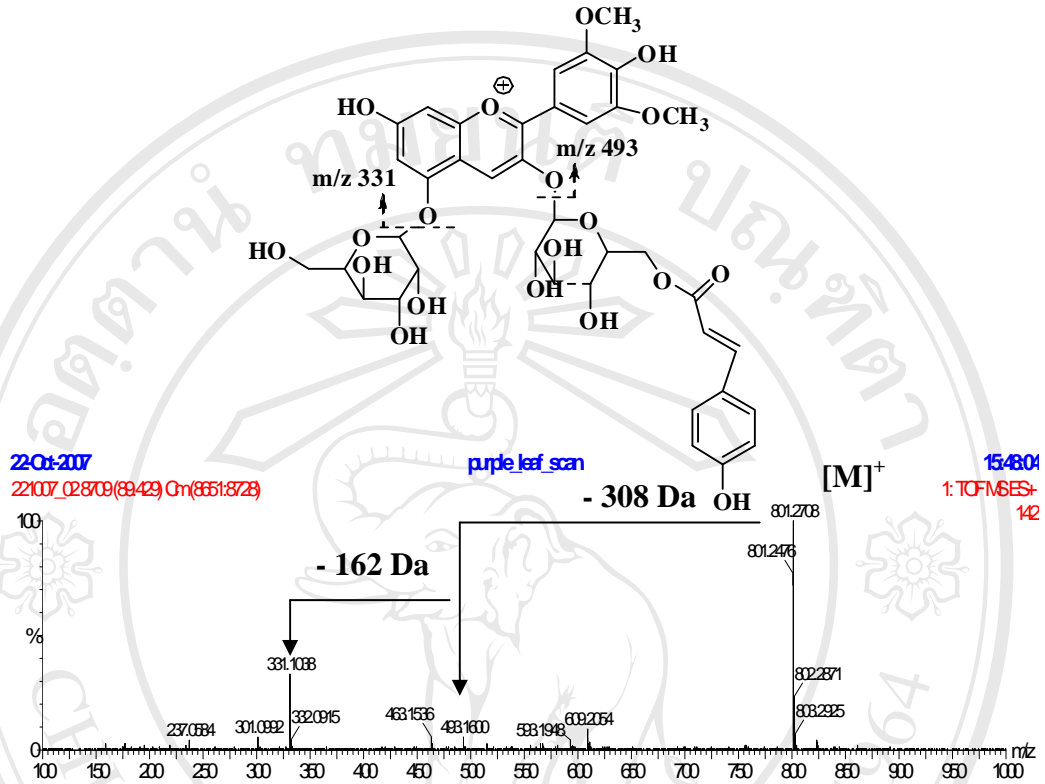


**Figure 3.48** Full scan mass spectra of an extract from the black rice cultivar Khumdoisakhet.

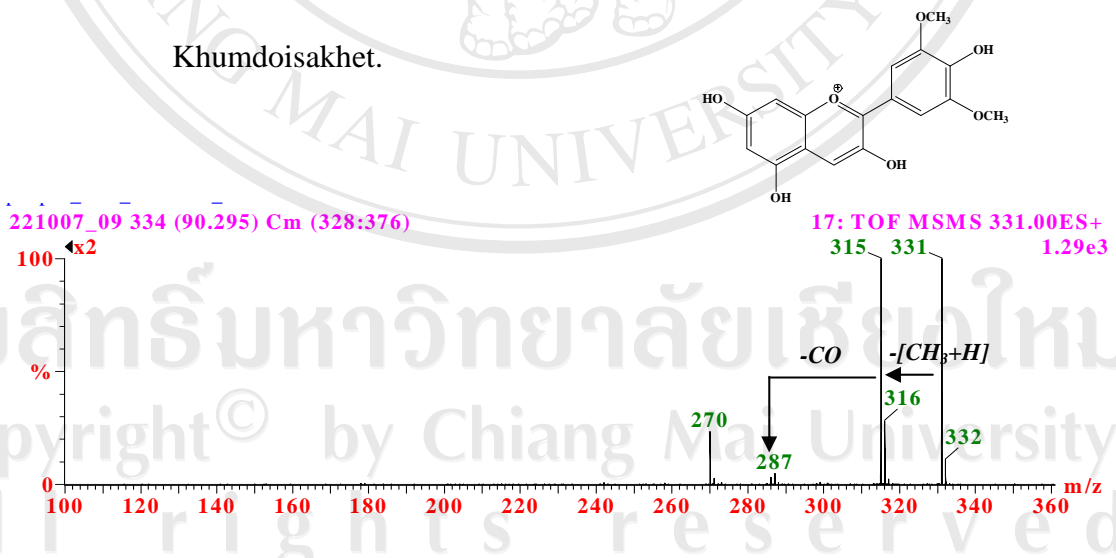
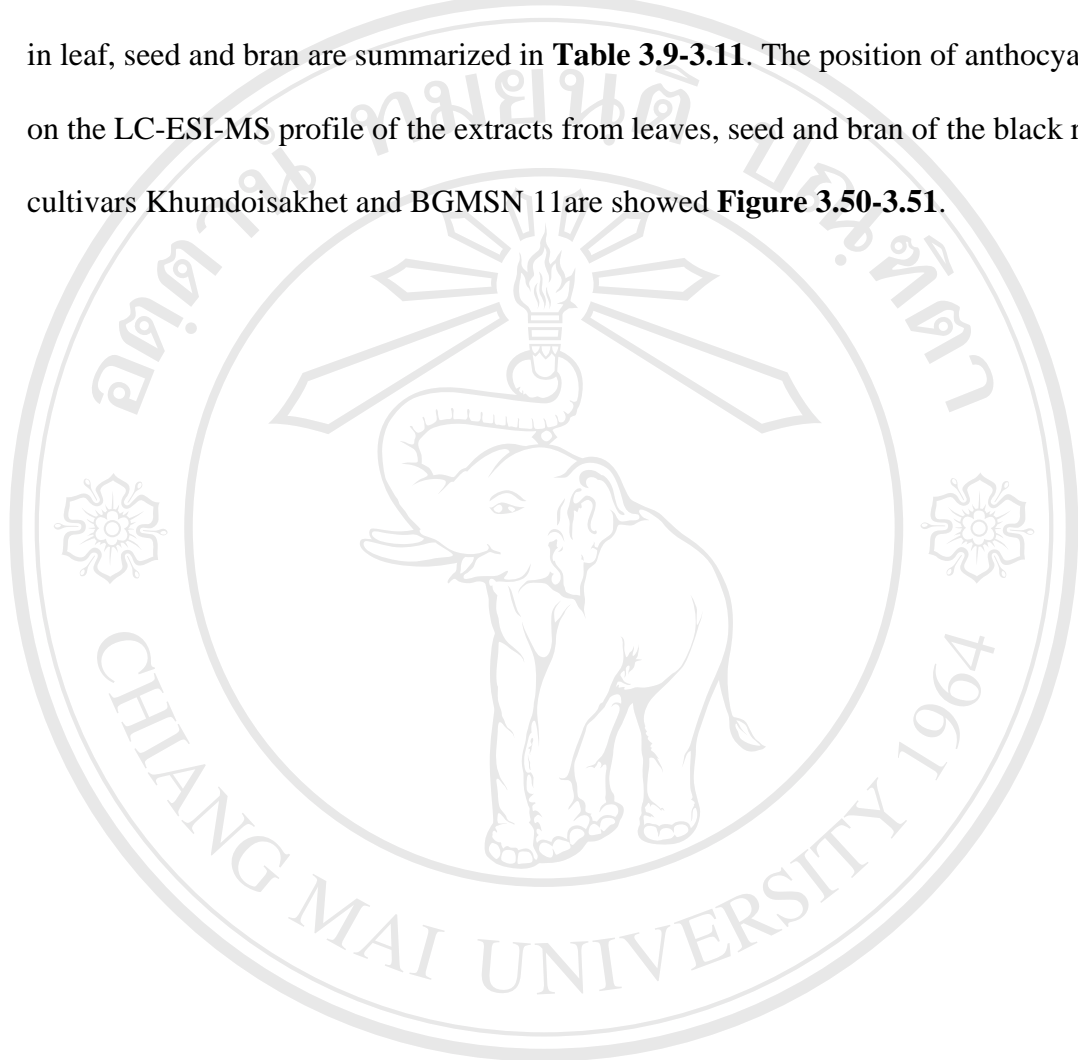


**Figure 3.49** MS/MS spectra of the parent ion at  $m/z$  331 obtained by LC-ESI-MS/MS

of the extracts from leaves of the black rice cultivar Khumdoisakhet showing fragmentation pathway of some ions as well as the neutral losses.

The mass spectrometric properties and identities of the black rice anthocyanins in leaf, seed and bran are summarized in **Table 3.9-3.11**. The position of anthocyanin on the LC-ESI-MS profile of the extracts from leaves, seed and bran of the black rices cultivars Khumdoisakhet and BGMSN 11 are showed **Figure 3.50-3.51**.



ลิขสิทธิ์มหาวิทยาลัยเชียงใหม่  
Copyright© by Chiang Mai University  
All rights reserved

**Table 3.9 Anthocyanins identified in leaves of the Thai black rice cultivar Khumdoisakhet and BGMSN 11**

Peak no.	Retention Time [min]	[M] <sup>+</sup> [m/z]	ESI <sup>(+)</sup> MS [m/z]	ESI <sup>(+)</sup> MS/MS [m/z]	compound
1	29.062	449	449 287	449 287	Cyanidin-3- <i>O</i> -glucoside
2	38.839	595	595 581	595 449 287	Cyanidin-3- <i>O</i> -glucoside-5- <i>O</i> -rhamnoside
3	42.769	463	463 301	463 301	Peonidin-3- <i>O</i> -glucoside
4	50.526	581	581	581 563 545 524 516 433	Cyanidin-3- <i>O</i> -xyloside glucoside
5	52.124	581	581	581 563 545 515 473 461	Cyanidin-3- <i>O</i> -xyloside glucoside (isomer)
6	56.925	611	611 449	611 449 287	Cyanidin-3- <i>O</i> -diglucoside
7	65.939	733	733 449 287	773 449 287	Cyanidin-3- <i>O</i> -diglucoside-5- <i>O</i> -glucoside
8	72.009	757	757 449 287	757 611 449 287	Cyanidin-3- <i>O</i> -( <i>p</i> -coumaroyl)glucoside-5- <i>O</i> -glucoside
9	72.202	787	787 625 287	787 625 433 287	Cyanidin-3- <i>O</i> -(feruloyl)glucoside-5- <i>O</i> -glucoside
10	75.027	625	625 463 433	625 463 445 343 301	Peonidin-3- <i>O</i> -diglucoside
11	88.916	801	801 493 331	-	Mavidin-3- <i>O</i> -( <i>p</i> -coumaroyl)glucoside-5- <i>O</i> -glucoside
12	92.032	741	741 493 331 219	741 463 301	Peonidin-3- <i>O</i> -( <i>p</i> -coumaroyl)glucoside-5- <i>O</i> -xyloside

**Table 3.10 Anthocyanins identified in seed of the Thai black rice cultivar Khumdoisakhet and BGMSN 11**

Peak no.	Retention Time [min]	MW	ESI <sup>(+)</sup> MS [m/z]	ESI <sup>(+)</sup> MS/MS [m/z]	compound
1	29.062	449	449 287	449 287	Cyanidin-3- <i>O</i> -glucoside
2	42.769	463	463 301	463 301	Peonidin-3- <i>O</i> -glucoside

**Table 3.11 Anthocyanins identified in bran of the Thai black rice cultivars Khumdoisakhet and BGMSN 11**

Peak no.	Retention Time [min]	MW	ESI <sup>(+)</sup> MS [m/z]	ESI <sup>(+)</sup> MS/MS [m/z]	compound
1	29.062	449	449 287	449 287	Cyanidin-3- <i>O</i> -glucoside
2	42.769	463	463 301	463 301	Peonidin-3- <i>O</i> -glucoside

Copyright © by Chiang Mai University  
All rights reserved

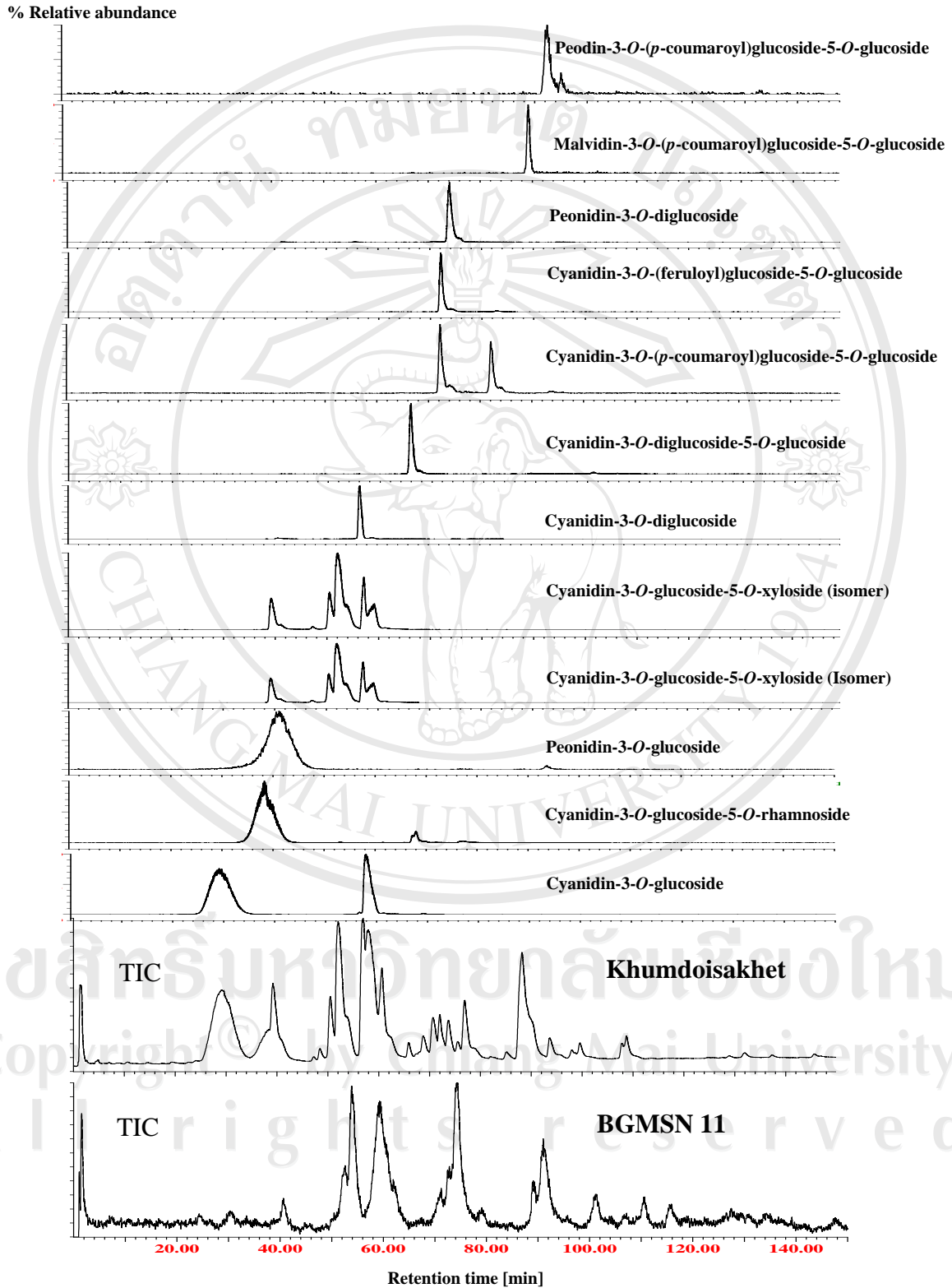


**Figure 3.50** Position of anthocyanins on the LC-ESI-MS profile of the extracts from leaves of the black rice cultivar Khumdoisakhet and BGMSN 11

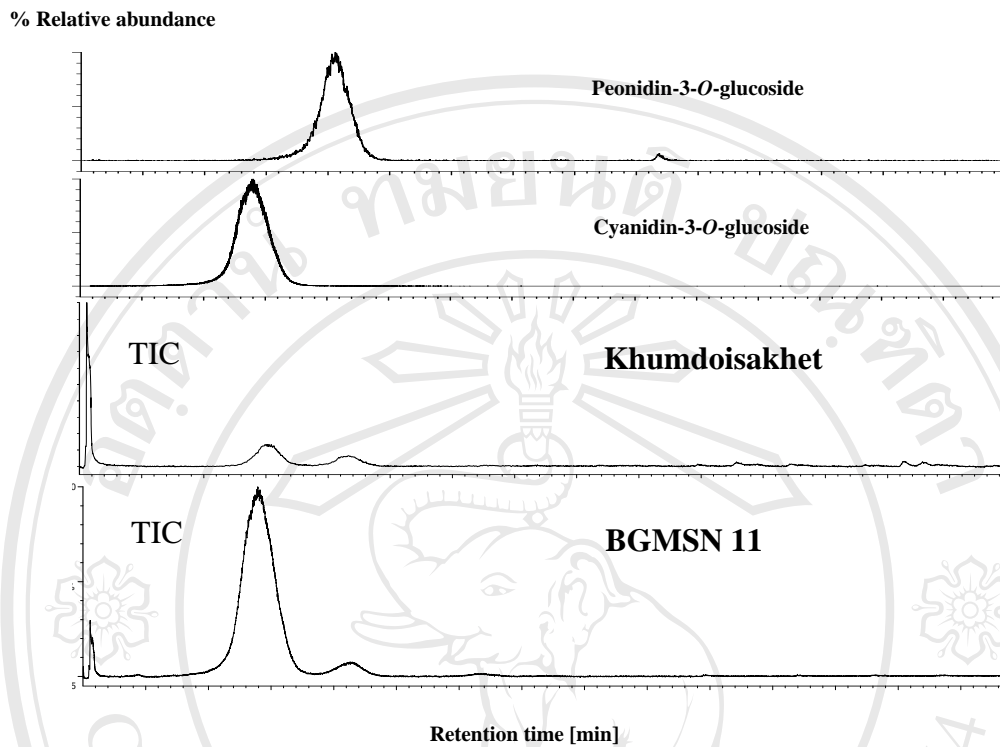


**Figure 3.51** Position of anthocyanins on the LC-ESI-MS profile of the extracts from seed of the black rice cultivar Khumdoisakhet and BGMSN 11

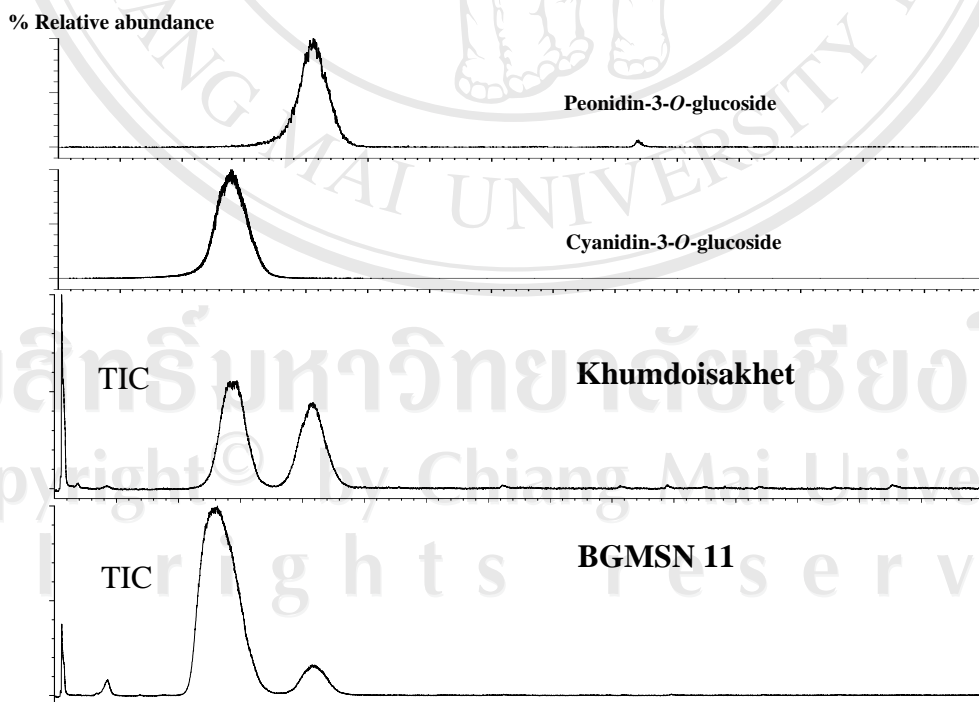


**Figure 3.52** Position of anthocyanins on the LC-ESI-MS profile of the extracts from bran of the black rice cultivar Khumdoisakhet and BGMSN 11

### **3.4 Relative contents of the identified anthocyanins in extracts of the black rices at different growth stages**

Contents of the identified black rice anthocyanins in leaves and seed obtained from BGMSN11 and Khumdoisakhet rice at different growth stages were determined by using LC-ESI-MS. Neutral red was used as internal standard. Peak area normalization method was utilized for calculation of the relative portions of an individual anthocyanin. The quantitative results of all identified anthocyanins in leaves and seed of BGMSN11 and Khumdoisakhet extracts at different growth stages are listed in **Table 3.12-3.15**.

Comparison of the contents in leaves and seed at different growth stages of each anthocyanin between the two black rice cultivars, Khumdoisakhet and BGMSN11, is also presented in **Figure 3.53**.

**Table 3.12** % Relative contents of identified anthocyanins in leaves of BGMSN1 extracts at different growth stages

No	Anthocyanins	MW	Relative content of anthocyanins (%)				
			1 Seedling stage	2 Tillering stage	3 Booting stage	4 Milk grain stage	5 Maturation stage
1	Cyanidin-3- <i>O</i> -glucoside	449	0.00	0.00	0.00	0.00	0.00
2	Cyanidin-3- <i>O</i> -glucoside-5- <i>O</i> -rhamnoside	595	0.00	0.00	0.00	0.00	0.00
3	Peonidin-3- <i>O</i> -glucoside	463	0.00	0.00	0.00	0.00	0.00
4	Cyanidin-3- <i>O</i> -xyloside glucoside	581	3.78	38.42	12.65	18.56	23.58
5	Cyanidin-3- <i>O</i> -xyloside glucoside (isomer)	581	7.70	12.76	19.56	19.61	18.92
6	Cyanidin-3- <i>O</i> -diglucoside	611	2.86	5.09	9.24	3.53	4.78
7	Cyanidin-3- <i>O</i> -( <i>p</i> -coumaroyl)glucoside-5- <i>O</i> -glucoside	757	9.21	12.81	19.57	14.40	4.08
8	Cyanidin-3- <i>O</i> -(feruloyl)glucoside-5- <i>O</i> -glucoside	787	2.89	3.95	9.17	4.98	3.99
9	Peonidin-3- <i>O</i> -diglucoside	625	1.26	3.73	2.98	2.15	3.03
10	Peonidin-3- <i>O</i> -( <i>p</i> -coumaroyl)glucoside-5- <i>O</i> -xyloside	741	4.74	4.91	5.39	6.97	3.29

**Table 3.13** % Relative contents of the identified anthocyanins in leaves of Khumdoisakheth extracts at different growth stages

No	Anthocyanins	MW	Relative content of anthocyanins (%)				
			1 Seedling stage	2 Tillering stage	3 Booting stage	4 Milk grain stage	5 Maturation stage
1	Cyanidin-3- <i>O</i> -glucoside	449	35.80	24.01	18.69	24.07	35.97
2	Cyanidin-3- <i>O</i> -glucoside-5- <i>O</i> -rhamnoside	595	17.15	6.15	5.70	6.48	41.99
3	Peonidin-3- <i>O</i> -glucoside	463	1.26	3.35	4.28	2.87	11.67
4	Cyanidin-3- <i>O</i> -xyloside glucoside	581	2.83	14.77	13.59	14.64	0.34
5	Cyanidin-3- <i>O</i> -xyloside glucoside (isomer)	581	6.42	12.20	10.45	10.44	1.32
6	Cyanidin-3- <i>O</i> -diglucoside	611	4.43	7.29	3.56	4.41	1.40
7	Cyanidin-3- <i>O</i> -( <i>p</i> -coumaroyl)glucoside-5- <i>O</i> -glucoside	757	11.29	2.98	2.77	2.68	0.00
8	Cyanidin-3- <i>O</i> -(feruloyl)glucoside-5- <i>O</i> -glucoside	787	1.86	3.36	3.20	2.58	0.00
9	Peonidin-3- <i>O</i> -diglucoside	625	4.63	6.17	15.91	1.18	0.62
10	Peonidin-3- <i>O</i> -( <i>p</i> -coumaroyl)glucoside-5- <i>O</i> -xyloside	741	5.01	1.41	2.30	2.09	0.20

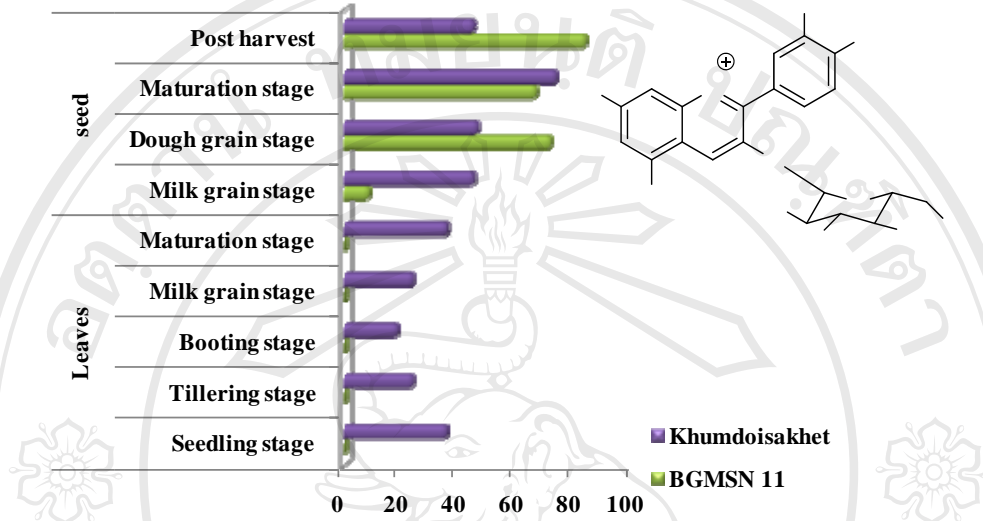
**Table 3.14** % Reative contents of the identified anthocyanins in seed of BGMSN1 extracts at different growth stages

No	Anthocyanins	MW	Relative contents of anthocyanins (%)			
			1	2	3	4
			Milk grain stag	Dough grain stage	Maturation stage	Post harvest
1	Cyanidin-3- <i>O</i> -glucoside	449	8.71	71.85	66.79	83.99
2	Cyanidin-3- <i>O</i> -glucoside-5- <i>O</i> -rhamnoside	595	37.00	1.09	2.40	0.56
3	Peonidin-3- <i>O</i> -glucoside	463	3.79	21.99	22.62	15.45
4	Cyanidin-3- <i>O</i> -xyloside glucoside	581	0.00	0.00	0.00	0.00
5	Cyanidin-3- <i>O</i> -xyloside glucoside (isomer)	581	0.00	0.00	0.00	0.00
6	Cyanidin-3- <i>O</i> -diglucoside	611	0.00	0.00	0.00	0.00
7	Cyanidin-3- <i>O</i> -( <i>p</i> -coumaroyl)glucoside-5- <i>O</i> -glucoside	757	0.00	0.14	0.00	0.00
8	Cyanidin-3- <i>O</i> -(feruloyl)glucoside-5- <i>O</i> -glucoside	787	0.00	0.08	0.31	0.00
9	Peonidin-3- <i>O</i> -diglucoside	625	3.97	0.09	0.66	0.00
10	Peonidin-3- <i>O</i> -( <i>p</i> -coumaryl)glucoside-5- <i>O</i> -xyloside	741	4.94	0.41	0.36	0.00

**Table 3.15** % Relative contents of identified anthocyanins in seed of Khumdoisakhet extracts at different growth stages

No	Anthocyanins	MW	Relative contents of anthocyanins (%)			
			1	2	3	4
			Milk grain stag	Dough grain stage	Maturation stage	Post harvest
1	Cyanidin-3- <i>O</i> -glucoside	449	45.27	46.43	73.79	45.14
2	Cyanidin-3- <i>O</i> -glucoside-5- <i>O</i> -rhamnoside	595	16.50	30.91	0.93	6.44
3	Peonidin-3- <i>O</i> -glucoside	463	10.94	18.16	21.15	42.60
4	Cyanidin-3- <i>O</i> -xyloside glucoside	581	0.00	0.00	0.00	0.00
5	Cyanidin-3- <i>O</i> -xyloside-glucoside 9isomer)	581	0.00	0.00	0.00	0.00
6	Cyanidin-3- <i>O</i> -diglucoside	611	0.00	0.00	0.00	0.00
7	Cyanidin-3- <i>O</i> -( <i>p</i> -coumaroyl)glucoside-5- <i>O</i> -glucoside	757	0.00	0.00	0.00	0.00
8	Cyanidin-3- <i>O</i> -(feruloyl)glucoside-5- <i>O</i> -glucoside	787	0.00	0.00	0.00	0.00
9	Peonidin-3- <i>O</i> -diglucoside	625	6.89	0.24	0.00	0.00
10	Peonidin-3- <i>O</i> -( <i>p</i> -coumaroyl)glucoside-5- <i>O</i> -xyloside	741	1.21	0.00	0.00	0.00

Cyanidin-3-*O*-glucoside



Peonidin-3-*O*-glucoside

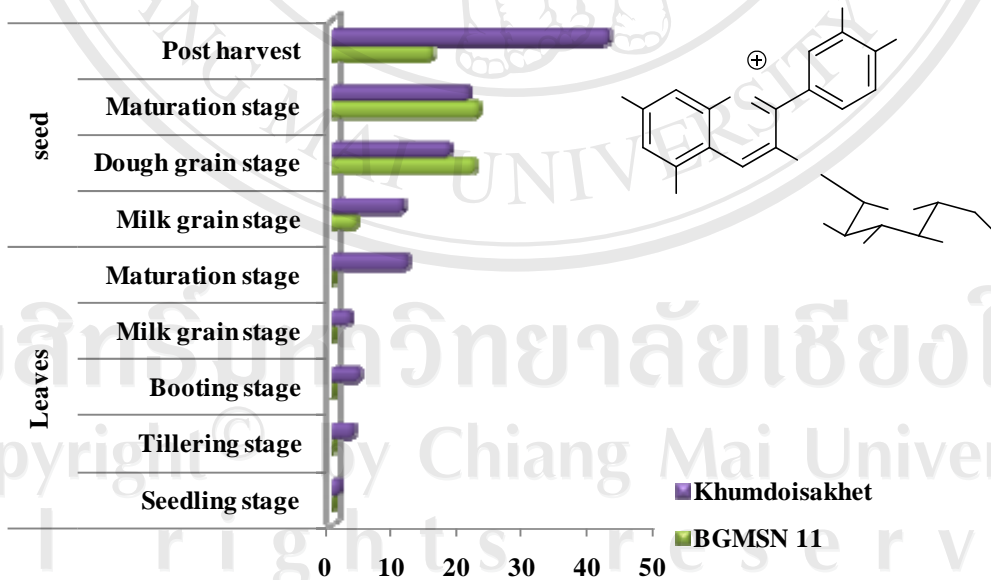
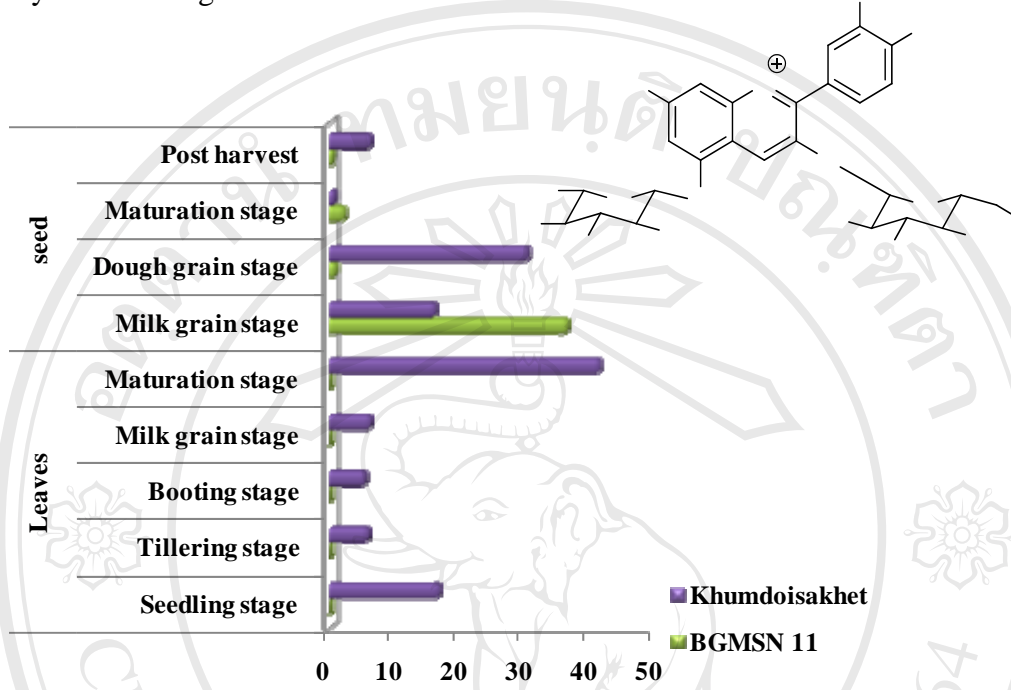


**Figure 3.53** Relative contents of anthocyanins obtained by LC-ESI-MS of the extracts from leaves and seed at different growth stages of the black rice cultivars Khumdoisakhet and BGMSN 11.

Cyanidin-3-*O*-glucoside-5-*O*-rhamnoside



Cyanidin-3-*O*-xyloside glucoside

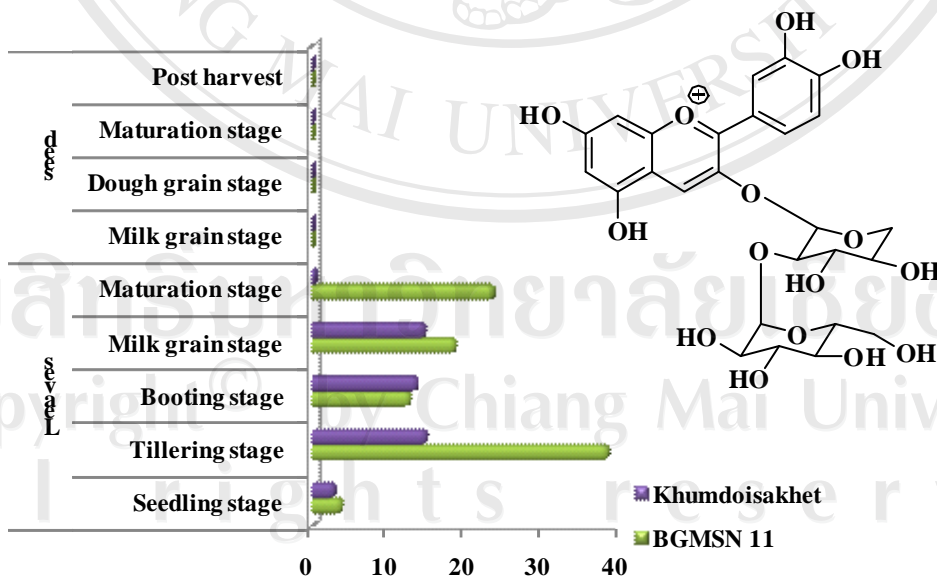
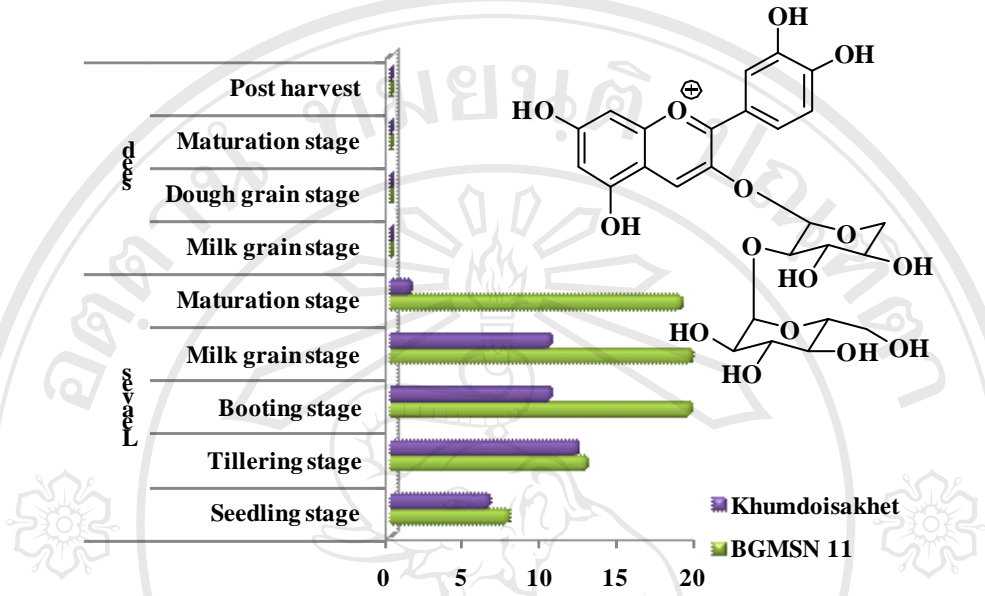


Figure 3.53 (Continues)

Cyanidin-3-*O*-xyloside glucoside (isomer)



Cyanidin-3-*O*-diglucoside

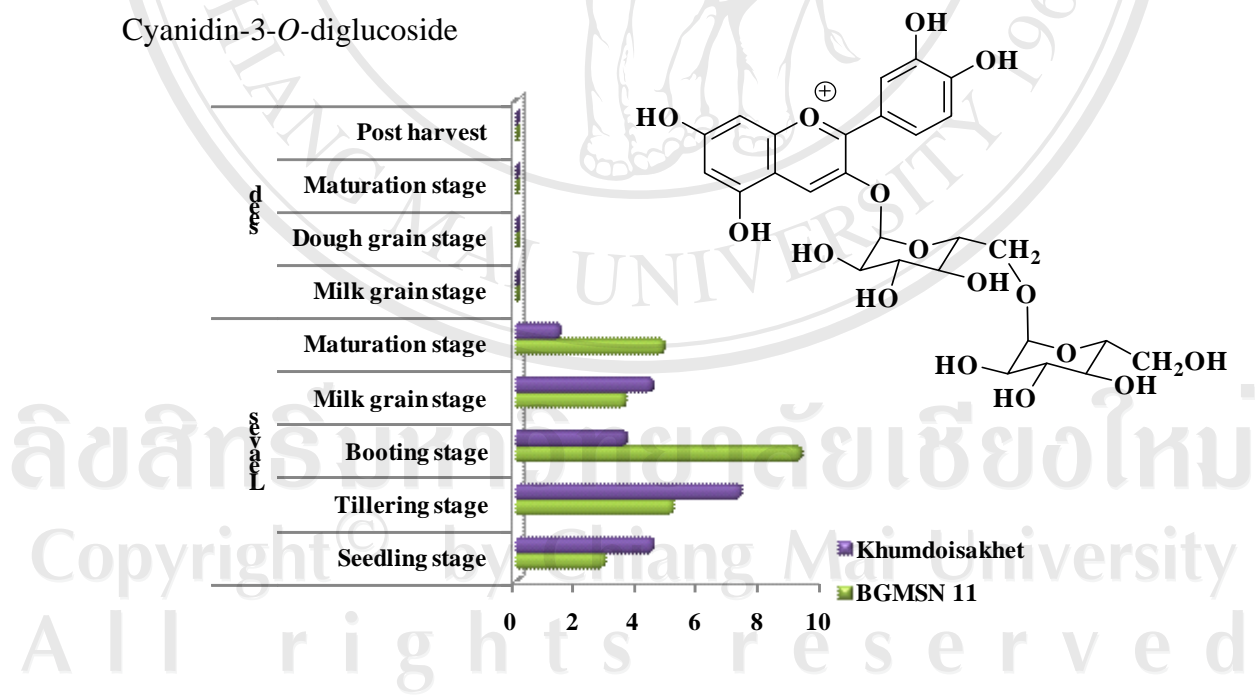


Figure 3.53 (Continues)

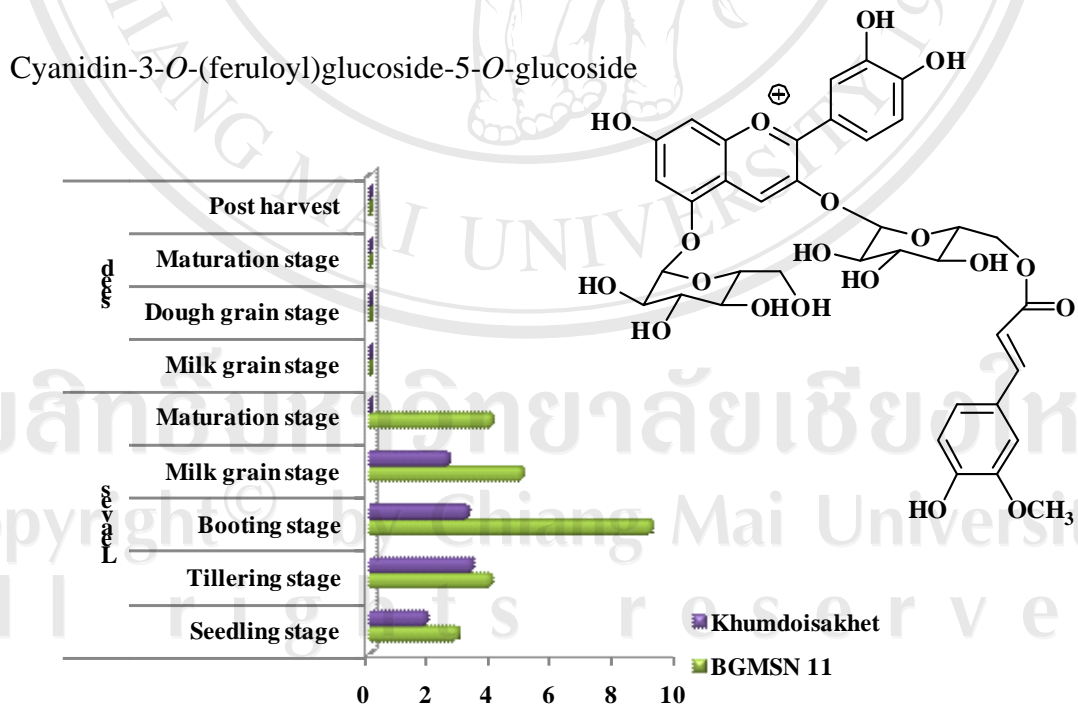
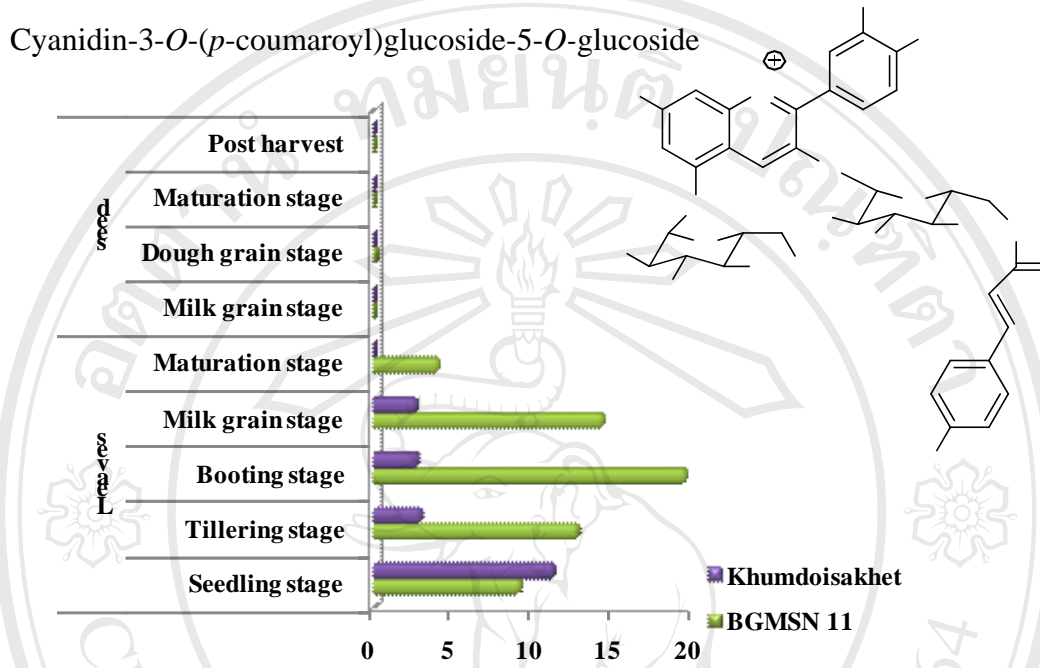
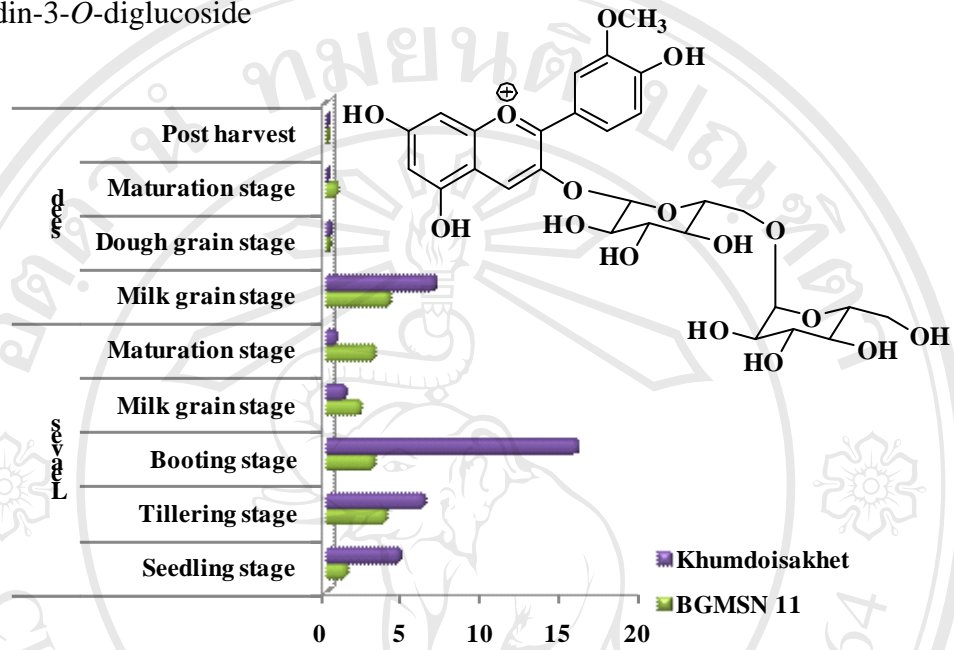


Figure 3.53 (Continues)

Peonidin-3-*O*-diglucoside



Peonidin-3-*O*-(*p*-coumaroyl)glucoside-5-*O*-xyloside

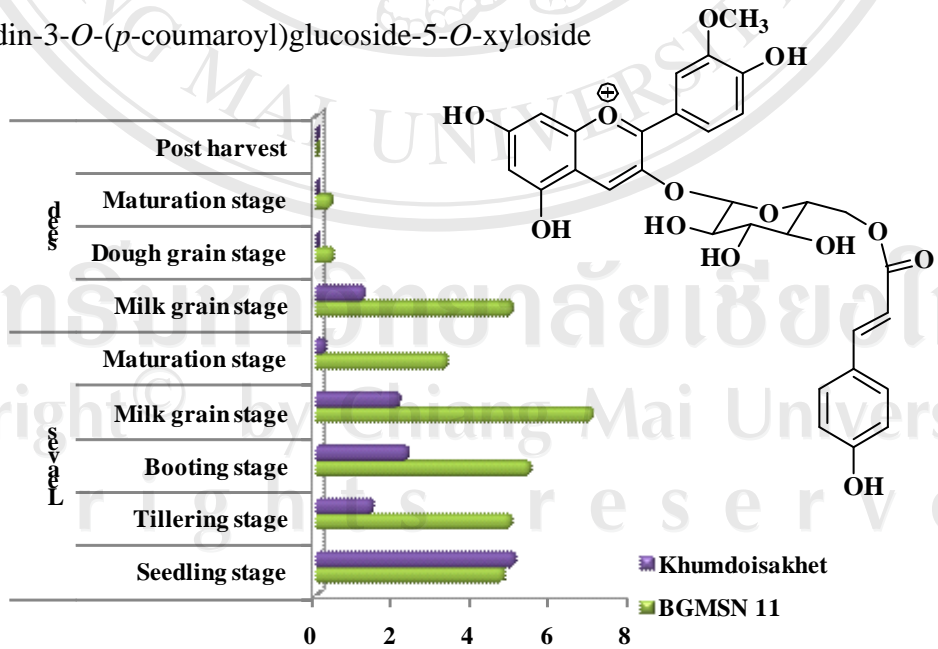


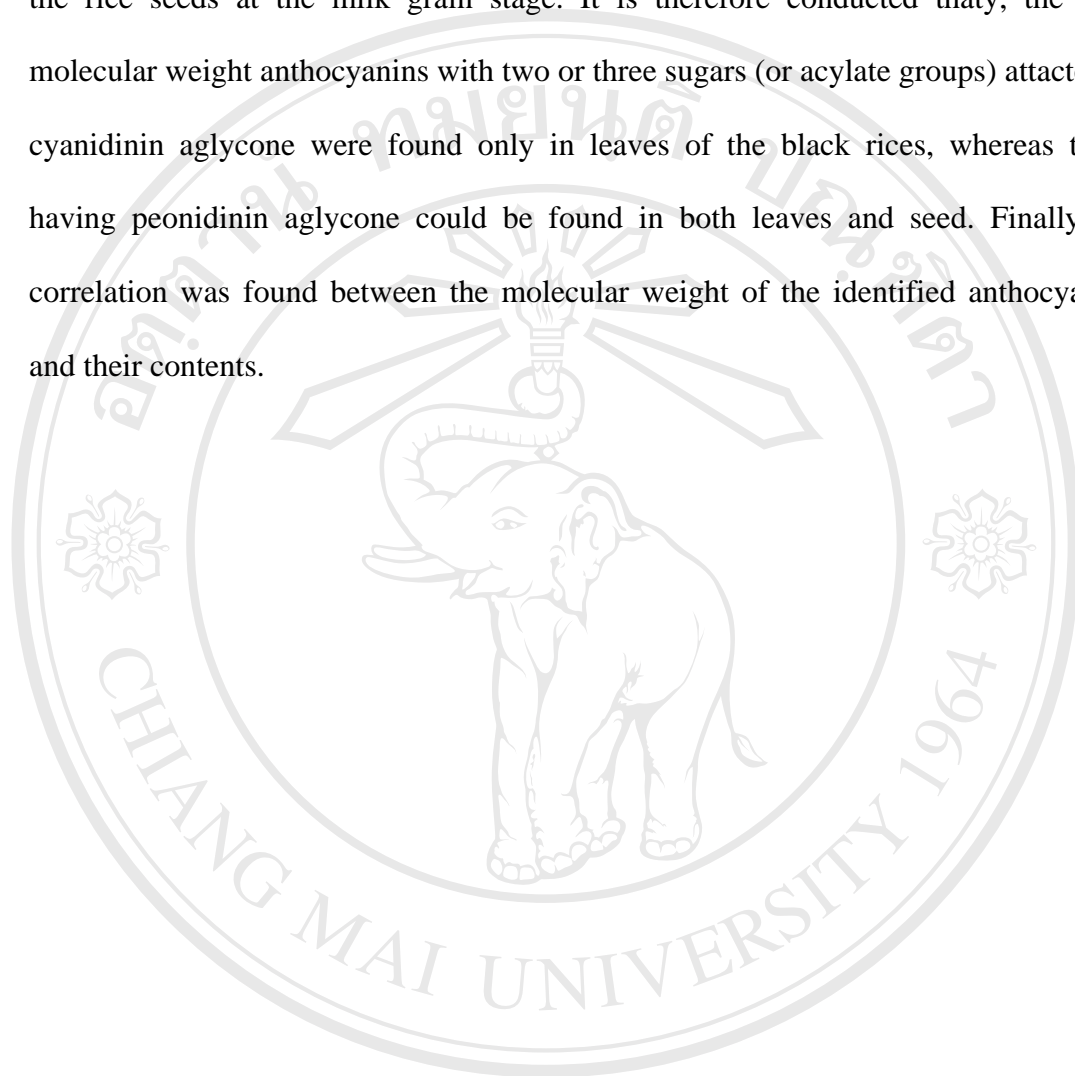
Figure 3.53 (Continues)

Of the twelve anthocyanins identified in the rice cultivars, Kumdoisakheth and BGMSN 11, cyanidin-3-*O*-glucoside, peonidin-3-*O*-glucoside and cyanidin-3-*O*-rutinoside were found only in seeds of both black rices. Their relative contents varied increasingly from the milk grain, dough, until maturation stage, except for cyanidin-3-*O*-rutinoside that was found at the highest content in maturation stage. It is noted that both cyanidin-3-*O*-glucoside and peonidin-3-*O*-glucoside are phytopigments having red and red-blue color, respectively, so they are responsible for the dark purple – black color of the rice brans. These two anthocyanins, cyanidin-3-*O*-glucoside and peonidin-3-*O*-glucoside, were also presented as pigments only in the leaf of Kumdoisakheth rice, that made its leaf color purple when compared with the green leaves of the cultivar BGMSN 11.

The black rice anthocyanins having two and three sugars (or acylate groups) such as cyanidin-3-*O*-xyloside glucoside, cyanidin-3-*O*-xyloside glucoside (isomer), cyanidin-3-*O*-diglucoside, cyanidin-3-*O*-(*p*-coumaroyl)glucoside-5-*O*-glucoside and cyanidin-3-*O*-(feruloyl)glucoside-5-*O*-glucoside, were not found in seed of both black rice cultivars. Their contents varied in leaves with similar pattern, increasing from seedling to booting stage and decreasing from milk grain to maturation stage. The reduction of these higher molecular weight anthocyanins started at the same time of seed production indicated their translocation from leaves to seeds with the reduction of a number of sugars in the molecules.

However, there were two high molecular weight anthocyanins, peonidin-3-*O*-diglucoside and peonidin-3-*O*-(*p*-coumaroyl)glucoside-5-*O*-xyloside, which were found in both leaves and seed of the two black rices. Their contents were highest in

the rice seeds at the milk grain stage. It is therefore conducted thaty, the high molecular weight anthocyanins with two or three sugars (or acylate groups) attached to cyanidin aglycone were found only in leaves of the black rices, whereas those having peonidin aglycone could be found in both leaves and seed. Finally, no correlation was found between the molecular weight of the identified anthocyanins and their contents.



ลิขสิทธิ์มหาวิทยาลัยเชียงใหม่

Copyright© by Chiang Mai University

All rights reserved